ADDIS ABABA UNIVERSITY

COLLEGE OF TECHNOLOGY AND BUILT ENVIRONMENT

SCHOOL OF CHEMICAL AND BIO ENGINEERING

VALORIZATION OF POLYETHYLENE TEREPHTHALATE WASTE INTO ACTIVATED CARBON FOR USED COOKING OIL PURIFICATION

A Thesis Submitted in Partial Fulfillment of the Requirements for the Award of Degree of Master of Science in Chemical Engineering (Environmental Stream)

By

Abdusemed Seid

Thesis Advisor: Dr. Shimelis Kebede

June 2025

Addis Ababa, Ethiopia

Approval Page

This is to certify that the thesis prepared by Mr. Abdusemed Seid, entitled "**Valorization of Polyethylene Terephthalate Waste into Activated Carbon for Used Cooking Oil Purification**," has been submitted as partial fulfillment of the requirements for the degree of Master of Science in Chemical Engineering (Environmental Stream). It complies with the university regulations and meets the accepted standards for content, quality, and originality.

Approved by the Examining Board:

Chairman, School's	_____	_____
Graduate Committee	Signature	Date
Dr. Shimelis Kebede	_____	_____
Advisor	Signature	Date
Dr. Sintayehu Nibret	_____	_____
External Examiner	Signature	Date
Dr. Kumsa Delessa	_____	_____
Internal Examiner	Signature	Date

Declaration

I declare that this thesis, titled " **Valorization of Polyethylene Terephthalate Waste into Activated Carbon for Used Cooking Oil Purification**," is the result of my own research and efforts toward my MSc degree. It has not been submitted, in whole or in part, for any other academic degree or professional qualification. I have acknowledged all sources of information through appropriate references.

Abdusemed Seid _____ _____

Signature Date

Abstract

This study focused on producing AC from post-consumer polyethylene terephthalate (PET) bottles for the purification of Used Cooking Oil (UCO), addressing two critical environmental concerns: plastic waste and oil pollution. AC was prepared using a double activation method with potassium hydroxide (KOH) at 800°C for 2 hours. The optimal sample was produced at an impregnation ratio of 1:1 (KOH to PET), resulting in a BET surface area of 984.9 m^2/g. Comprehensive characterization was conducted using BET and BJH analyses, X-ray diffraction (XRD), Fourier transform infrared spectroscopy (FTIR), scanning electron microscopy (SEM), energy-dispersive X-ray spectroscopy (EDX), and thermogravimetric analysis (TGA). The adsorption process was optimized for free fatty acid (FFA) removal, achieving a maximum efficiency of 68.2% under conditions of 112 minutes of contact time, a 7.5% (w/v) adsorbent dosage, and a mixing speed of 240 rpm. Under these conditions, the oil's peroxide value (PV) was reduced by 77.21%, and lightness increased by 3.51 units. Kinetic modeling revealed that the adsorption followed a pseudo-second-order model with an R^2 value of 0.9657. However, the pseudo-first-order (R^2 = 0.9644) and intraparticle diffusion (R^2 = 0.9522) models also demonstrated reasonable fits. The PET-derived AC exhibited competitive, and in some cases superior, performance compared to biomass-based alternatives, indicating its potential as a sustainable and effective material for UCO purification.

Key Words: Adsorption, Activated Carbon, Polyethylene Terephthalate, Used Cooking Oil, Free Fatty Acid, Optimization, Kinetic Study

Acknowledgements

First and foremost, I thank the Almighty Allah for guiding me throughout this journey. Next, my special gratitude goes to my advisor, Dr. Shimelis Kebede, whose extraordinary guidance and personal commitment went far beyond what is expected. His support played a vital role in the success of not only this work but also in my academic and personal development. I also thank Professor Ahmed Mustefa from the Department of Computational Chemistry for his belief in me. His contributions made this journey possible. I would also like to appreciate all my teachers, laboratory technicians and school of chemical and bio engineering staff for their continuous efforts in the growth of their students. Lastly, I would like to thank my family, in particular my mother, Asiya Hussein, for her love, prayers, and all the sacrifices she has made.

Table of Contents

List of Tables

List of Figures

List of Abbreviations and Acronyms

Abbreviation and Acronyms	Full Term
AC	Activated Carbon
ANOVA	Analysis of Variance
BBD	Box-Behnken Design
CV	Coefficient of Variance
FFA	Free Fatty Acid
IPD	Intraparticle Diffusion
PET	Polyethylene Terephthalate
PFO	Pseudo-First-Order
PSO	Pseudo-Second-Order
PV	Peroxide Value
RSM	Response Surface Methodology
SSA	Specific Surface Area
UCO	Used Cooking Oil

1. Introduction

1.1. Background

PET is a widely used semi-amorphous plastic. Its mechanical strength, chemical resistance, and transparency are the main factors that qualify it for packaging food and beverages (Nisticò, 2020). The global production of PET in 2022 was approximately 56 million tons (Soong et al., 2022). PET is burned or dumped since it is hard to degrade. PET wear does not bio degrade thus remains in environment for centuries eventually breaking down into harmful micro plastics that have grave ecological consequences (Pereira et al., 2024).

The PET sector in Ethiopia will witness an impressive compound annual growth rate of 14.74% that will reach 16.72% in 2029 on the account of rising requirements in packaging, textiles, and consumer goods (Singh, 2023). Increase of plastic waste including PET bottles as a significant portion results to about 3,300 $\mathrm{ton/d}$ is also experienced by Addis Ababa (Kogyo Co, 2024). However, the waste management system within the city remains poor which results to pollution blockage of drainage systems and risk flood water. Disposing off PET waste improperly can result into various environmental issues such as soil infertility, nutrient depletion and health risks to people due to diseases vectors proliferation system (Tesfaye., 2020).

Among the conventional waste disposal techniques such as landfilling and incineration, environmental issues arise from land use, leachate contamination, toxic emissions as well as greenhouse gasses production (Zhou, 2021). Therefore, recognized are recycling methods. Mechanically recycling by washing and extrusion is cost-effective though constrained by quality of products (Santomasi et al., 2024). Biological recycling applies enzymes to depolymerize plastics which need to be researched further in order for commercial application to be possible (Hiraga et al., 2019; Muringayil Joseph et al., 2024). Chemical recycling which involves carbonization, thermal cracking and solvolysis is able to change PET waste into valuable products. Particularly carbonization manufactures AC useful for environmental remediation purposes (Blanchard & Mekonnen, 2024). The current investigation centers in the carbonization of PET waste with a view of producing ACs that can be used in treating UCO system.

Additionally, UCO poses an environmental and public health threat as well. In Ethiopia used oils are either extensively or in untreated ways reused mainly or discharged into the environment if it is particularly in informal food sectors with accumulated major health risks (Nurhazirah et al., 2019). Biomass based-ACs have a good performance on the quality improvement of UCO through removal of contaminants such as FFA impurities and moisture content in recycled oil towards its safety usability (Arman et al., 2024; Gustaman et al., 2020).

The goal of this study is to transform waste plastic bottles into AC and evaluate this process for the purification of UCO in Ethiopia; which are two imperatives to address two critical environmental challenges in Ethiopia.

1.2. Problem Statement

PET is among a widely used plastic polymers globally for packaging and bottling applications. If they are not disposed properly, they end up in water bodies, affecting the aquatic habitat. Groundwater is becoming contaminated with PET plastic and the products leached from it. It can also end up in landfills, where the decomposition requires centuries. Due to the hazardous disposal of plastic waste, the land is becoming infertile. Soil nutrients are being depleted, which restricts plant growth and decreases productivity. Micro-sized and nano-sized particles of PET plastic have raised serious concerns regarding potential dangers and risks to nature and human well-being. (Dhaka et al., 2022).

Ethiopia currently consumes about 386,000 tons of plastic annually. However, due to insufficient technology, investment, and expertise, only 30–40% of this plastic waste is recycled African (African Association of Entrepreneurs, 2020). In Ethiopian cities, especially Addis Ababa, urban waste is significantly composed of PET bottles (Tesfaye., 2020). PET, primarily used for water and soda bottles, accounts for 41% of the total plastic waste generated in the city (Natural Resources Stewardship Program [NatuReS], 2021). Accumulated PET wastes block drainage systems and flooding while ruining the overall look of the land. In addition, it damages human health by facilitating the proliferation of disease-carrying organisms.

The other environmental and human health threat is UCO. Its volume is increasing with the growing demand for cooking oil. Similar to other developing countries, UCOs are treated as waste in Ethiopia and repeatedly fried without any concern from users or relevant authorities.

Continual heating and oxidation breaks down triglycerides into peroxides, FFAs, and aldehydes that cause gastrointestinal, cardiovascular, liver diseases and are carcinogenic (Nurhazirah et al., 2019). It contains hydrocarbons that can make the land more toxic and decrease its fertility and productivity (Olanrewaju Alade et al., 2022). Discharge of UCO into the waters can also destroy and harm aquatic life by affecting the process of photosynthesis (Nurhazirah et al., 2019).

Recent researches have shown that PET waste can be chemically transformed into AC. But, there has been limited or no study on the use of PET-derived AC for purifying UCO, especially within the Ethiopian context.

This study attempts to fill this gap by formulating and investigating the performance of PET-based ACs for UCO purification. It is expected to address the Ethiopian context of integrated sustainable AC engineering and resource recovery from waste cooking oil.

1.3. Objectives

1.3.1. General Objective

The general objective of this research was to valorize PET waste into AC for the purification of UCO.

1.3.2. Specific Objectives

- To assess the methods of AC from PET waste, including carbonization and activation techniques.
- To study the physicochemical and thermal properties of the AC produced from PET waste, including surface area, pore size distribution, structural property, functional groups, elemental composition, and thermal stability.
- To optimize the removal efficiency of FFA from UCO using PET-derived AC through RSM.
- To identify the adsorption kinetics of FFA removal and identify the most suitable kinetic model.

1.4. Significance of the Study

This research aimed to bring environmental, scientific, and societal essence. By turning these materials into useful resources and reusable goods, it offers a workable way to reduce plastic waste and used oil pollution in an environmentally friendly way. Scientifically, the research advances the development of low-cost AC from synthetic polymers. This provide insights into material science and adsorption technology. From societal point of view, it enhances public health by potentially decreasing the circulation of toxic, UCOs. Not only this, but also it offers economic relief through the production of affordable purification media.

Furthermore, this study promotes circular economy principles by demonstrating how waste materials can be transformed into functional products. Hence, reliance on virgin materials and waste generation will be minimized.

1.5. Scope of the Study

To achieve the specific objectives, the research was conducted within the following scope. AC was prepared by optimizing three methods and two impregnation ratios. Further characterization was performed on the best product. The characterization includes Brunauer–Emmett–Teller (BET) analysis for SSA, Barrett–Joyner–Halenda (BJH) analysis along with N2 adsorption-desorption isotherm for pore characterization, Scanning Electron Microscope (SEM) analysis for surface morphology, X-Ray Diffraction (XRD) analysis for structural properties, Fourier Transform Infrared Spectroscopy (FTIR) analysis for functional groups, Energy-Dispersive X-Ray Spectroscopy (EDX) Analysis for elemental composition, and Thermogravimetric Analysis (TGA) for thermal properties.

The effectiveness of the adsorbent and the statistical optimization of the removal efficiency of FFA were determined. The optimization of removal efficiency was conducted using RSM with a BBD. For the optimum condition, additional characterizations, including PV, and color analyses were performed.

Additionally, the study investigates the adsorption kinetics of FFA removal. The kinetic study was carried out by applying widely accepted kinetic models: PFO, PSO and IPD, to understand the rate and mechanism of adsorption. This study, therefore, offers a practical and innovative method to tackle both plastic and used oil.

2. Literature Review

2.1. Overview of Plastic Waste

One of the most significant environmental problems is plastic waste considering how fast global plastic intake has grown and how long plastics last in ecosystems. Plastics production spiked since the 1950s to over 330 million metric tons annually in all parts of the globe by 2016 (Geyer et al., 2017). Despite being widely utilized in various applications on a global scale only so little as less than nine percent gets reused and instead fills up landfills or natural environments for hundreds of years to come (Geyer et al., 2017). Plastic are very slow degraders which break into microplastics that even further contaminate water, soil, air leading to risks of wildlife and human health (Wright & Kelly, 2017). The impacts on environment through plastic waste are wide ranging nature. In marine setting for example debris made by plastics affects organisms physically interfering with their ingestion or trapping them within its confines it may also destroy habitat or transport foreign species (Jambeck et al., 2015). On land, plastics alter soil properties and microbial communities, reducing soil fertility and affecting agricultural productivity (Rillig, 2012). Furthermore, improper disposal methods such as open burning release toxic chemicals and greenhouse gases, contributing to air pollution and climate change. Developing countries face particular challenges in managing plastic waste due to limited infrastructure and resources. This often results in widespread pollution in urban and rural areas, worsening environmental degradation and public health risks (Lebreton & Andrady, 2019). Therefore, addressing plastic pollution requires integrated strategies that improve waste collection, promote recycling technologies, and encourage sustainable consumption.

2.2. PET as a Carbon Source

PET is a type of polyester plastic. It is produced through the polymerization of terephthalic acid and ethylene glycol. As an alternative, it can also be produced by the transesterification of dimethyl terephthalate with ethylene glycol (Soong et al., 2022). PET possesses excellent combination of properties, like mechanical strength, thermal stability, and chemical resistance (Balamurugan et al., 2021).

The carbon content of PET is approximately 62.5% by weight. Therefore, it is a suitable carbon source for the preparation of AC (Yuliusman et al., 2017). Another characteristic of PET precursor is its melting point. Its melting point ranges from 250 to 260°C. This property allows

chemically impregnated raw PET to dry at a temperature of 105°C for 24 hours without melting. The other important characteristics is its consistent structure and composition, which make it an ideal raw material for AC preparation. In addition to these, its large accumulation in the environment makes it a cost-effective raw material (Efimov et al., 2024).

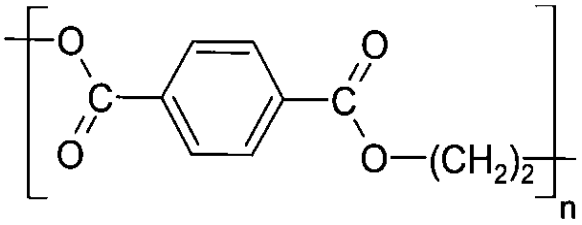

Figure 2.1: Chemical structure of PET

2.3. Overview of UCO

Globally, 50 megatons of UCO are produced, and only 14.1 megatons of it are recycled (Beghetto, 2025). This implies that significant amount of UCOs is directly discharged to the environment. When UCOs are disposed of in the environment, they create numerous problems. Among these, blockages in urban sewer systems that lead to overflowing sanitary sewers, clogged sewers and septic systems, and an unnecessary increase in the organic load on water bodies. UCOs have been linked to significant health risks, including heart disease, stroke, Parkinson's disease, Alzheimer's disease, liver disease, gastrointestinal disorders, and even mutagenesis in the human body (Legesse, 2020).

UCOs are leftovers of oils and fats that have been used for frying purposes (Legesse, 2020). During frying, oils are exposed to high temperatures, usually (150–190 ℃). It is important to note that frying is a very complex process in which heat and mass transfer phenomena occur between the food and the frying oil. As a result, the food dehydrates, absorbs oil, and releases some of its lipids into the frying medium (Abrante-Pascual et al., 2024). Vegetable oils break down when reused for frying, resulting in adverse effects on their physical and chemical properties. Frying a cooking oil multiple times causes lipid oxidation and peroxide formation. It also reduces the quantity of unsaturated fatty acids while increasing both color intensity and FFA levels (N.J.T et al., 2020).

FFAs are long-chain carboxylic acids. When oils are exposed to high temperatures, the triglycerides begin to hydrolyze and form FFAs, which leads to rancidity (Nurulain et al., 2021). Therefore, FFAs are commonly regarded as key indicators of oil degradation.

Consequently, this research aims to optimize the removal of FFAs, while other indicators are characterized solely under these optimal conditions. Figure 2.2. shows the general chemical structure of FFA molecules, where R is a hydrocarbon chain.

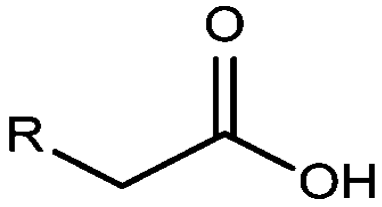

Figure 2.2: Representative structure of FFAs

2.4. UCO Purification Methods

The purification of UCO is generally achieved using physical, or chemical methods (Hendi et al., 2021). Basic techniques such as sedimentation and filtration are among the most widely used physical methods. However, these only address suspended solids and large particles. For dissolved impurities like FFAs and peroxides, physical methods are ineffective. (Khuzaimah & Eralita, 2020). On the other hand, the chemical refining method of UCO involves mixing the oil with an alkali solution (Hendi et al., 2021). Although this method is effective, saponification reaction will take place. As a result, there is loss of neutral oil and secondary waste is generated. In contrast, combined physicochemical methods are more effective for purifying UCO.

Table 2.1: Comparison of purification methods for UCO

Method	**Effectiveness**	**Limitations**
Physical	Effective for removing suspended solids and large particles	Ineffective for dissolved impurities like FFAs and peroxides
Chemical	Effective for removing FFAs and other chemical impurities	Causes saponification, loss of neutral oil, and generates secondary waste
Physicochemical	Effective for removing FFAs, peroxides, and color without altering oil chemically	Efficiency depends on adsorbent properties; requires optimization

Therefore, physicochemical method, particularly adsorption, stands out as an effective method for treating UCO. Because, they remove impurities like FFA, and peroxides without altering the oil chemically (Azzena et al., 2023). This method efficiently removes degradation products

while preserving the oil's nature. Additionally, it is environmentally friendly, and straightforward to implement (Azzena et al., 2023). Its applicability makes the method promising approach for large scale UCO treatment (Ojo & Awogbemi, 2024).

2.5. Adsorption

One of the most widely used physicochemical method for UCO purification is adsorption (Jasmidi et al., 2023). Adsorption is a physicochemical process by which an adsorbate (the substance being adsorbed) adheres to the surface of an adsorbent (the material on which adsorption occurs) (Dali et al., 2023). In this process, the undesirable components of the UCO are adsorbed onto the adsorbent, enabling their removal along with the adsorbent (Vuorte et al., 2020). It is suitable for removing a wide range of degradation compounds, including FFAs, and PV. Unlike chemical neutralization, adsorption does not chemically change the oil. It also does not generate toxic secondary products. This makes the method more sustainable and environmentally friendly (Sukmawati & Sunarto, 2021). In addition to this, adsorption processes are generally cost-effective, easy to operate, and highly efficient (Karume et al., 2023).

A variety of adsorbents have been explored, including clay minerals such as bentonite and attapulgite, natural polymers like chitosan and starch, and bio-derived ACs from materials such as banana peels, coconut shells, and cocoa husks. The most commonly used adsorbent is AC (Jasmidi et al., 2023).

2.6. AC

AC is a highly porous, amorphous carbon material. Its ability to adsorb substances makes it one of the most promising methods for the sustainable purification of UCO. Because, it adsorbs the impurities without decomposing or reacting after use (Jasmidi et al., 2023). ACs with good physicochemical characteristics are known for their good adsorption capacity (Heidarinejad et al., 2020). And the physicochemical characteristics are dependent on the type of precursor used (Njewa et al., 2022). According to different studies, PET-derived ACs have many superior characteristics compared to biomass-based ACs. Therefore, PET-based AC can be considered as one of the best adsorbents for liquid waste management such as purification of UCO.

2.7. Preparation Methods of AC

AC preparation involves a process of activation. The activation methods are classified in to two categories. These are physical and chemical activation methods (Heidarinejad et al., 2020).

2.7.1. Physical Activation

Physical activation is the simplest method for the production of AC (Shahcheragh et al., 2023). This method involves carbonization and activation consecutively. The carbonization stage involves simple pyrolysis in a neutral atmosphere, while activation is done using oxidizing agents like carbon dioxide, and steam. For carbonization, a relatively low temperature, between 450 and 600°C is required. On the other hand, in the activation stage higher temperatures, ranging from 800 to 1100°C are employed (Heidarinejad et al., 2020).

Even if this method is the most commonly used method, it comes with its own advantages and disadvantages. Process simplicity, quick activation, and suitability for large scale production are among the advantages of this method (Shahcheragh et al., 2023). Besides, the method is relatively cheap and environmentally friendly due to absence of chemicals. However, it has a lot of drawbacks. The first problem is its large amount of energy consumption (Blanchard & Mekonnen, 2024). The other limitation is that it is difficult to control the flowrate of the activation agent (Shahcheragh et al., 2023). As a result, the surface chemistry of the AC becomes less desirable. Physical activation predominantly enlarges existing pores rather than forming new ones, which limits the development of well-defined microporosity (Phothong, Tangsathitkulchai, & Lawtae, 2021). Additionally, as burn-off progresses beyond approximately 50%, pore merging and collapse begin to dominate, degrading the pore structure (Takeda et al., 2023). Therefore, physical activation is less suitable technique for this study. Because, the purification of UCO relies on enhanced surface chemistry.

2.7.2. Chemical Activation

In contrast, in chemical activation, chemical substances are used to develop porous AC. Among the chemical activators used, sulfuric acid (H_2SO_4), phosphoric acid (H_3PO_4), potassium hydroxide (KOH), sodium hydroxide (NaOH), potassium carbonate (K_2CO_3), and zinc chloride ($ZnCl_2$) can be mentioned (Blanchard & Mekonnen, 2024). This method consists three main steps. These are impregnation, heat treatment, and final washing. Unlike the physical method, carbonization and activation may occur either simultaneously or successively. Temperature

and impregnation ratio are major parameters that define the quality of produced AC. The temperature used is usually between 400 and 900°C. On the other hand, impregnation ratio is adjusted to get an AC with better physicochemical characteristics (Shahcheragh et al., 2023).

Like other methods, chemical activation has its own benefits and trade-offs. Compared to physical method, it yields an AC with higher surface area and improved pore structure. Its relatively low temperature requirement is another advantage (Blanchard & Mekonnen, 2024). This method also offers higher production efficiency than that of the physical method (Shahcheragh et al., 2023). Long washing step requirement to remove chemical residuals is a disadvantage of this method. Because, the washing process in turn generate waste that can be harmful to the environment.

Table 2.2: Merits and demerits of activation methods

Activation Method	Merits	Demerits
Physical	Simple, avoids chemical usage, suitable for large-scale production	Gives limited surface functionality
Chemical	Yields a higher surface porosity and better control of surface chemistry	Involves chemicals, needs thorough washing, may generate chemical waste

Based on the comparisons above, chemical activation is preferred over physical activation. The benefits of double chemical activation outweigh the drawbacks of increased energy consumption as it results a better surface porosity. Additionally, it is important to consider the proper disposal of residual chemicals.

2.7.2.1. Direct Chemical Activation

Direct chemical activation is a method in which a carbonaceous raw material is impregnated with a chemical activating agent. The heat treatment after the impregnation is carried out in an inert atmosphere. The temperature typically ranges between 400 and 900°C. Even though the method is efficient in yielding high surface area AC, it needs extensive washing to remove residual chemicals (Heidarinejad et al., 2020).

2.7.2.2. Indirect Chemical Activation

In indirect chemical activation, carbonization and activation occur as two separate processes. First, the carbon precursor is carbonized to produce a char. Next, the char is activated using a selected activating agent. This method allows for better control over pore development than

the direct activation. Therefore, the produced AC has good properties, that makes it suitable for specific applications. However, the process needs longer time. And its yield is compared to direct activation (Heidarinejad et al., 2020).

2.7.2.3. Double Chemical Activation

Double chemical activation involves two chemical treatments. The first treatment follows the same procedure as direct activation. Then, the second treatment, which is the reactivation step follows. Compared to both direct and indirect activation methods, this one results in AC with a significantly improved surface area and pore distribution. Promising results are being shown even if the method is young (Zhang et al., 2024).

2.8. Factors Affecting Activated Carbon Preparation

2.8.1. Effect of Precursor

The precursor strongly influences the yield and porosity of activated carbon. Agricultural residues, nutshells, and synthetic polymers are commonly used (Ioannidou & Zabaniotou, 2007). In this research, PET is selected as the precursor due to its high carbon content and availability as a plastic waste stream, making it both cost-effective and environmentally beneficial (Yahya et al., 2015).

2.8.2. Effect of Temperature

Activation temperature controls pore development and surface area. Moderate to high temperatures (700 - 900 °C) enhance microporosity, whereas excessively high values may cause pore collapse and reduce yield (Lua & Yang, 2004). Therefore, 800 °C is applied in this study as it is widely reported as an optimum point to balance carbon yield and pore structure (Rodríguez-Reinoso, 1997).

2.8.3. Effect of Time

Activation time determines the extent of burn-off. Longer times increase surface area but may over-widen pores and reduce structural stability (Lua & Guo, 1999). In this research, 2 hours was selected as it allows sufficient pore development while preventing over activation and yield loss, consistent with prior findings (Molina-Sabio & Rodríguez-Reinoso, 2004).

2.8.4. Effect of Impregnation Ratio

The mass ratio of activating agent to precursor dictates the porosity level. Low ratios under-activate, while very high ratios collapse pores and lower yield. Optimized ratios provide well-developed micro/mesopores (Jagtoyen & Derbyshire, 1998; Molina-Sabio & Rodríguez-Reinoso, 2004). Thus, the impregnation ratio is carefully adjusted in this research to maximize adsorption capacity.

2.9. Factors Affecting Adsorption of degradation products from UCO Treatment

Several factors determine the effectiveness of AC in removing pollutants from UCO. Previous studies have shown that the adsorption process is affected by AC dosage, contact time, mixing speed, treatment temperature, and particle size. In this work, the influence of three factors, namely contact time, AC dosage, and mixing speed are studied.

2.9.1. Effect of Contact Time

The contact time between the AC and the UCO plays a huge role in the removal of pollutants. Longer adsorption times results a higher reduction of the acid number (Harianingsih et al., 2023). However, Harianingsih et al., (2023) also demonstrated that adsorption beyond the optimal time leads to desorption, causing the impurity levels to rise again. Miskah et al., (2019) observed that optimal adsorption using durian peel based AC occurred after 150 minutes of contact time, with no significant improvements observed thereafter. Similarly, according to Sukmawati & Sunarto, (2021) , the highest adsorption efficiency of activated charcoal was 49.97% for reducing peroxide number and 50.11% for reducing FFA were obtained after 3 hours.

2.9.2. Effect of AC Dosage

AC dosage is another factor that determines the effectiveness of adsorption process. A higher dosage enhances the removal of impurities by increasing the number of available active sites for adsorption. Bostan et al., (2024) concluded that the amount of adsorbent (eggshell) affects the acid value and PV of used sunflower oil. According to the result, higher removal was achieved for a higher dose. Likewise, Arman et al., (2024) shown that maximum removals of FFA and peroxide were attained when the adsorbent to adsorbate ratio is 15% (w/v).

2.9.3. Effect of Mixing Speed

Mixing speed affects the dynamics of interaction between the AC and the oil. For example, Abdul Hamid et al., 2016 made clear that stirring speed must be controlled for a better removal efficiency. On another research, Harianingsih et al., 2023 also used a constant speed of 200 rpm to carry out the adsorption of UCO. This indicates that uncontrolled mixing speed has significant influence on the adsorption efficiency.

2.10. Applications

AC is an adsorbent, which is widely used for various purposes. One of its application area is environmental remediation. Its properties can vary based on the raw materials and activation methods employed. But, the variation allows it to be used for multiple applications targeted different types of pollutants. From large-scale industrial purification systems to small laboratory setups, AC has become a key method for promoting a cleaner environment (Tadda et al., 2016).

One of the most remarkable ability of AC is that it can remove different pollutants. For instance it serves as an effective adsorbent for heavy metals, organic compounds, and dyes in waste water treatment (Saleem et al., 2019). Moreover, AC can be applied for the elimination of contaminants, such as pesticides and herbicides (Soonmin & Kabbashi, 2021). Beyond waste treatment, AC can serve as a catalyst to extract liquid hydrocarbon fuel from post-consumer plastics. Generally, its capacity to capture and retain these unwanted substances is vital to protect human health safe. It also helps to maintain ecosystem functions. AC's effectiveness in purifying UCO is being studied recently.

Once UCO is purified, it has various applications in different areas. For instance, a UCO with low level of FFA and PV can be used as a key ingredient to make liquid hand soap (Rahayu et al., 2024). Additionally, it is used as a biodiesel raw material in the energy sector. And, for this particular application, the purification is necessary to avoid unwanted side reactions (Putra et al., 2014). Besides these applications, well-treated UCO can be mixed with stearin and natural essential oils to produce aromatherapy candles (Ramadhani et al., 2023). If safety standards are fulfilled, carefully treated UCO may also be utilized in the preparation of animal feed and energy supplements (Nuru & Getachew, 2021). The present work aims to produce plastic based AC and test its effectiveness in removing pollutants from UCO so that the purified UCO is used for different applications.

2.11. Summary of Previous Research

2.11.1. PET Based AC

Recent studies have showed the growing interest in using PET as a precursor to produce AC. This interest comes from PET's carbon-rich composition, low cost, abundant availability, and its status as an environmental threat. Many researchers have used different methods to produce AC, which possess improved surface properties.

One of the most common method being used is physical activation. The process use oxidizing gases like steam and carbon dioxide (CO_2) as activating agent at high temperatures. For example, Pham, (2023) used physical activation with CO_2 and achieved a surface area of 703.4 m^2/g. The process involved carbonization of PET at 550°C and then followed by activation at 850°C. The total time for both operations was 40 minutes. Another researchers, Ali et al., (2014) used similar approach and got a much larger surface area of 2010 m^2/g. Considerably, the researchers used higher carbonization and activation temperatures of 650°C and 950°C, respectively compared to Pham's. Likewise, László & Szucs, (2001) applied physical method. However, they used CO_2 as an activating agent instead of steam. In their work, carbonization at 750°C was followed by activation at 900°C for 90 minutes. Their AC then possessed a surface area of 1170 m^2/g.

On the other hand, chemical activation can be carried out at a relatively lower temperature but uses strong chemical activators. Pereira et al., (2024) applied direct chemical activation using potassium hydroxide (KOH) 850°C for 60 minutes. The resulting AC attained a SSA of 1002 m^2/g. Some researchers also compared different activating chemicals. For instance, Blanchard & Mekonnen, (2024) tested different activators including H_3PO_4, H_2SO_4, and KOH that resulted in widely varied surface areas. Based on their report, 1223 m^2/g for phosphoric acid, 583 m^2/g for sulfuric acid, and 1338 m^2/g for KOH were obtained.

While physical activation can result in higher surface areas, as seen with Ali et al. (2014) reporting 2010 m^2/g, chemical activation often offers superior microporosity and improved surface functionalization (Pereira et al., 2024; Blanchard & Mekonnen, 2024). Chemical activation typically introduces oxygen-containing groups and a more favorable pore size distribution that enhances adsorption capacity and selectivity, especially for molecules like free fatty acids (Pham, 2023). This enhanced surface chemistry can compensate for the somewhat lower total surface area observed in this study's double chemical activation method.

Furthermore, chemically activated carbons tend to exhibit greater thermal stability and structural integrity compared to physically activated carbons (László & Szucs, 2001). These factors contribute to more efficient and selective adsorption in applications such as used cooking oil (UCO) treatment. Therefore, while the surface area metric favors physical activation, chemical activation may provide better performance considering pore structure and surface functionalities relevant to FFA removal.

2.11.2. Purification of UCO by AC Adsorption

A number of studies have been conducted on the purification of UCO using different biomass-based ACs. The main focus of these researches was on reducing FFA level, and PV. According to most of the researches, the adsorption effectiveness is dependent on factors like contact time and AC dosage.

Khuzaimah & Eralita, (2020) used AC from coconut shell to reduce the FFA and PV of a UCO. They obtained 37.5% FFA removal and 85.4% reduction in PV with a low AC dosage of 5% (w/v) and a short contact time of 15 minutes. On the other hand, Putra et al., (2014) observed a 53.1% FFA removal.. However, they didn't specify the precursor used for the AC and the contact time for the adsorption. A more extended contact time of 120 minutes was tested by Arman et al., (2024). In this test, a high dose of 15% (w/v) cocoa pod husk-based AC was used. Then, a 49.4% FFA removal and 2.3% reduction in PV was achieved. Even if it is not efficient result, it highlighted that it is possible to use agricultural wastes for UCO treatment. Another research by Suryandari & Kusuma, (2021) investigated the effectiveness of bamboo-based AC. Despite a low dosage of 1.33% (w/v), a longer contact time of 120 minutes, a FFA removal of 65.9% and a PV reduction of 62.8% were observed.

Collectively, these studies illustrate that the UCO purification performance of AC varies significantly with the material source, contact time, and dosage.

2.12. Research Gaps

A research gap exists in the literature regarding the valorization of post-consumer PET waste into AC for UCO purification. While AC from various biomass sources has been widely studied for oil purification, PET-based AC remains underexplored. Most prior research has addressed plastic waste management or oil purification in isolation, rather than integrating both

challenges into a sustainable solution. This gap is especially relevant in developing countries, where PET accumulation and improper UCO disposal pose significant environmental and public health concerns.

There is also a lack of systematic investigations into optimizing process parameters such as contact time, adsorbent dosage, and mixing speed for the effective use of PET-derived AC in UCO purification. Comparative studies evaluating the adsorption efficiency of PET-based AC against conventional biomass-based adsorbents for removing key oil contaminants, including FFAs and peroxides, are limited. Without such comparative data, the advantages and potential limitations of PET-based adsorbents remain unclear.

Most studies have been confined to laboratory-scale experiments, with insufficient attention to the scalability, economic feasibility, and environmental sustainability of implementing PET-derived AC in real-world applications. Additionally, there is a lack of research on the regeneration and reuse of these adsorbents, which is critical for sustainable waste management.

This study aims to address the research gap by investigating the production, characterization, and application of AC derived from PET waste for UCO purification. It will optimize key process parameters, evaluate adsorption performance relative to conventional alternatives, and assess the potential for practical implementation, particularly where both PET waste and UCO pollution are pressing issues.

3. Materials and Methods

3.1. Materials

3.1.1. Raw Materials

Post-consumer PET bottles were collected from households to serve as raw material for the production of AC. Additionally, UCO was gathered from food vendors and stored for further treatment and analysis.

3.1.2. Chemicals and Reagents

In this research, all chemicals used were of analytical reagent grade. Distilled water was used as a solvent in the preparation of AC, in FFA and PV analyses, for washing AC, and for other cleaning purposes. Ethanol (96%) was also served as a solvent for FFA and PV analyses, as well as a cleaning agent. KOH pellets (85%) were used both as an activating agent in the preparation of AC, and as a titrant for FFA analysis. Hydrochloric acid (35%) was utilized to adjust the pH of the produced ACs. For PV analysis, acetic acid (99%), chloroform, potassium iodide, sodium thiosulfate, and starch indicator were used. Phenolphthalein was used as the indicator for FFA analysis.

3.1.3. Apparatus and Equipment

In the preparation of AC, a muffle furnace, crucibles, a magnetic stirrer, and a vacuum filter were used. For characterizing the produced ACs, advanced equipment was employed. A Brunauer-Emmett-Teller (BET) surface area analyzer was used to determine SSA and pore volume. Another apparatus, Barrett-Joyner-Halenda (BJH) pore size distribution analyzer assessed mesopore size distribution. Surface morphology and functional groups were analyzed using a Scanning Electron Microscope (SEM) and a Fourier Transform Infrared Spectroscopy (FTIR), respectively. Additionally, a Thermogravimetric Analyzer (TGA) was employed to evaluate the thermal stability of the AC. Other equipment, including, scissors, beakers, flasks, measuring cylinders, test tubes, a water bath, a sonicating bath, a burette, micropipette, a pH meter, density meter, a mortar and pestle, an analytical balance, and an oven, were used at various stages of the research. A 45-micrometer syringe filter was also utilized to study the kinetics of adsorption.

3.2. Framework of the Research

The following diagram illustrates the research framework.

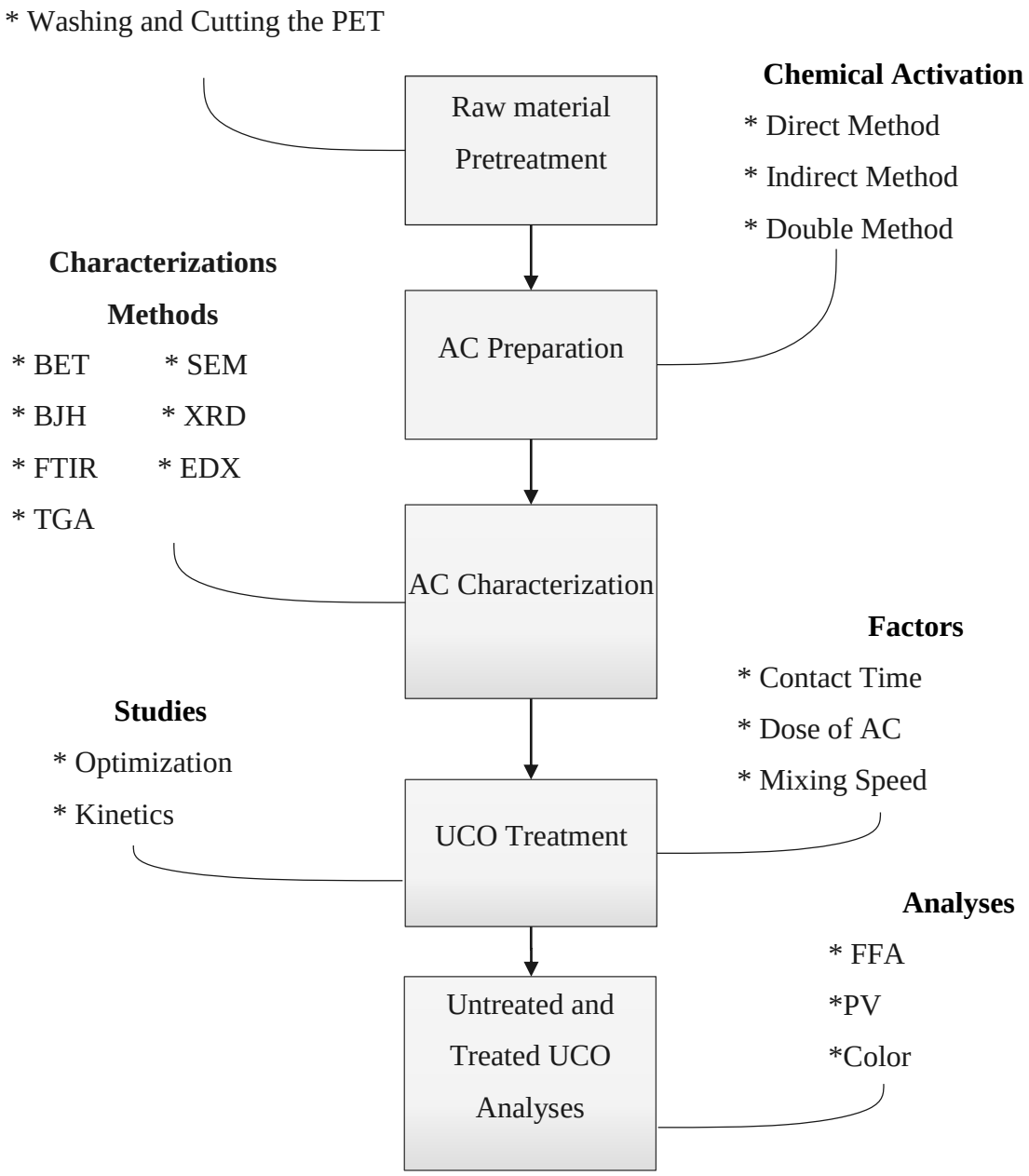

Figure 3.1: Framework of the research

3.3. Raw Material Treatment

3.3.1. PET Precursor

Post-consumer PET bottles were thoroughly washed with tap water to remove impurities. After drying in the sun, the bottles were cut into small pieces of approximately 0.5 cm x 0.5 cm using scissors.

3.3.2. UCO

The collected UCO was heated to 50°C to reduce its viscosity; after which it was filtered to remove large particles.

3.4. Preparation of AC

The preparation of PET-derived AC utilized three chemical activation methods: direct, indirect, and double activation. The direct and double activation methods were adapted from Blanchard & Mekonnen, (2024), while the double activation method is based on the approach described by Zhang et al., (2024). In all methods, the particle size of the products was fixed between the size of 100 μm and 125 μm. For instance, Jacobi Carbons emphasizes that granular AC used in vegetable oil treatments is manufactured with strictly controlled particle size distributions, often within the range of 100 to 150 μm, to ensure fast filtration and optimal adsorption kinetics (Jacobi Carbons, 2023). The activation and carbonization stages was performed at a temperature of 800°C and a holding time of 2 hours. This is because this temperature optimizes and facilitates pore development as KOH melts at 765°C effectively (Gao et al., 2018). Prolonged activation at this temperature ensures thorough chemical activation and improves adsorption properties while preventing pore collapse from higher temperatures or longer durations (Kuptajit, 2021). The yields of each preparation technique were also calculated using equation 3.1.

$$\% \text{ Yield} = \frac{m_{AC}}{m_{PET}} x100\% \quad \text{..... (3.1)}$$

Where:

m_{PET}= the mass of the precursor PET (g)

m_{AC}= the mass of the AC after washing (g)

3.4.1. Preparation through Direct Activation

First, an aqueous saturated KOH solution was prepared. A specific amount of PET pieces was measured and thoroughly mixed with this solution. The mixture was then dried in an oven at 105°C for 24 hours. After drying, the impregnated PET was transferred to a crucible and exposed for heating in the muffle furnace. The crucible was placed in the muffle furnace, where the temperature was set to 800°C, and the material was combusted for 2 hours. The resulting product was washed multiple times with a 0.5 M hydrochloric acid solution and then rinsed several times with distilled water until the pH reached nearly 7. After washing, the product was dried in an oven for an additional 24 hours. Finally, size reduction was performed, and the product was labeled as D, where D stands for direct activation.

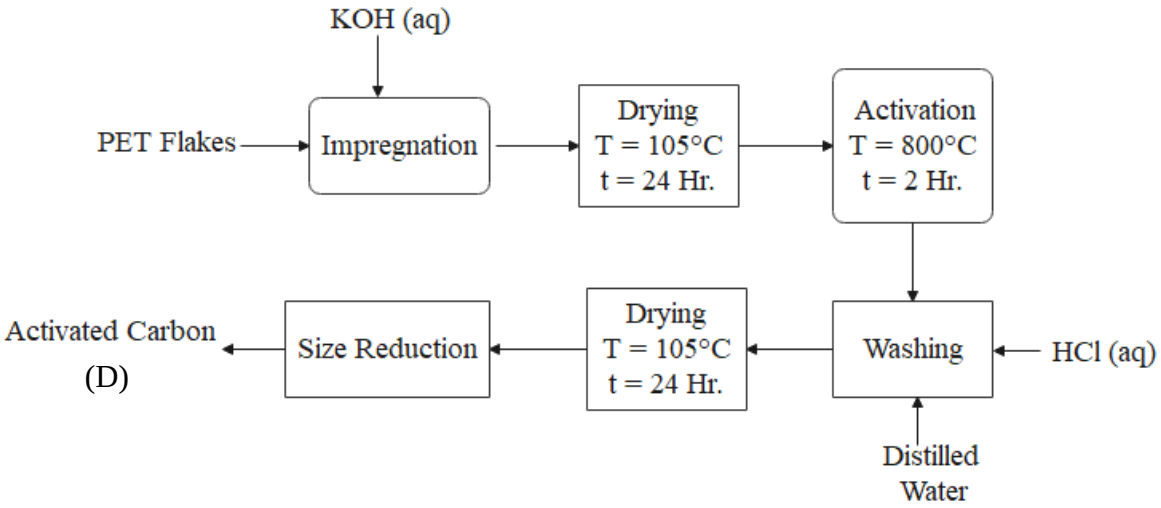

Figure 3.2: Process flow diagram for direct activation of PET with KOH

3.4.2. Preparation through Indirect Activation

In contrast to the direct method, the first step of the indirect activation process, after measuring the desired mass of PET, involves direct carbonization to create a synthetic char. During carbonization a temperature of 800°C and a duration of 2 hours were used. Following carbonization, the synthetic char was washed with distilled water until the washing water became clear to eliminate unwanted oxidation products. The char was then dried in an oven at 105°C for 24 hours.

Next, an appropriate concentration of aqueous KOH was prepared, and the dried char was impregnated with this solution. After impregnation, the sample was dried under the same

conditions as the char. The dried impregnated sample was then activated in a muffle furnace for 2 hours at 800°C. Subsequently, it was washed with 0.5 M hydrochloric acid and rinsed with distilled water. Finally, the dried product was ground and labeled as I, where I stands for indirect activation.

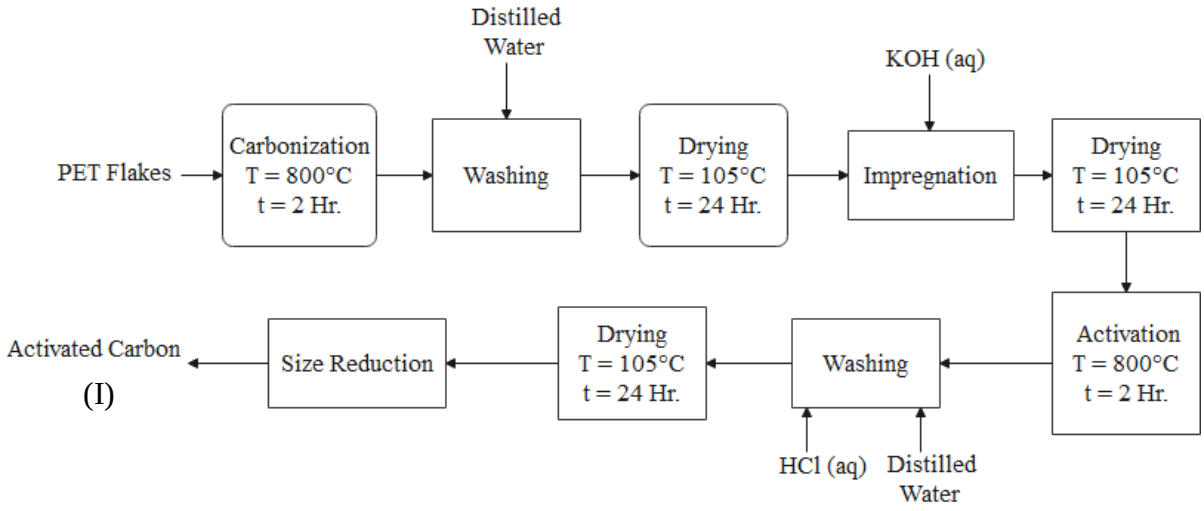

Figure 3.3: Process flow diagram for indirect activation of PET with KOH

3.4.3. Preparation through Double Activation

In this method, all steps used for direct activation were applied to the first activation, except for the size reduction step. For the second activation, an aqueous saturated KOH solution was prepared, and the AC from the first activation was re-impregnated. After drying at 105°C for 24 hours, the material was treated at 800°C for 2 hours in a muffle furnace, using a crucible. The resulting product was then washed multiple times with 0.5 M hydrochloric acid and thoroughly rinsed with distilled water to remove any residual base. Finally, after size reduction, the product was designated as X, where X stands for double chemical activation.

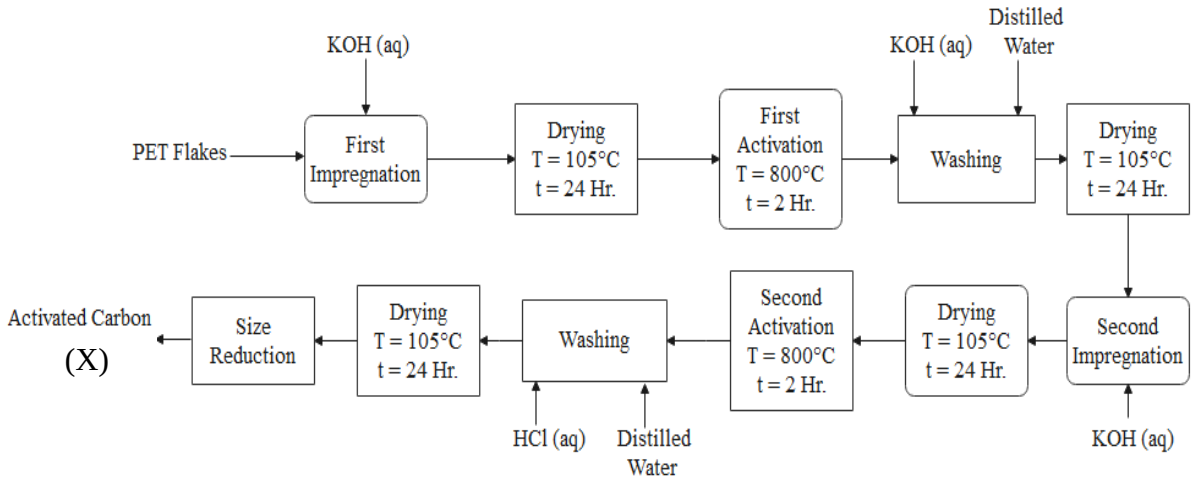

Figure 3.4:Process flow diagram for double activation of PET with KOH

3.5. AC Preparation Matrix

A PET char and five AC samples were prepared. All experiments maintained a carbonization and activation temperature of 800°C for 2 hours, while varying impregnation ratios were applied. For the direct and indirect methods, KOH to PET ratios of 1:1 and 2:2 were used. On the other hand, only a 1:1 ratio was employed for the double activation method because the crucibles were destroyed when a ratio of 2:1 were employed twice. The sample codes for the products are put in Table 3.1. below.

Table 3.1: Activation parameters and sample codes for the PET-derived ACs

Activation Method	Treatment Temperature (°C)	Treatment Duration (Hour)	Impregnation Ratio (KOH:PET)	Sample Code
-	800	2	-	C
Direct	800	2	1:1	D11
Direct	800	2	2:1	D21
Indirect	800	2	1:1	I11
Indirect	800	2	2:1	I21
Double	800	2	1:1	X11

3.6. Characterization of AC

Seven different characterizations were conducted to evaluate the quality of the AC samples. A Brunauer-Emmett-Teller (BET) surface area analyzer was used to determine the SSA and pore volume, while a Barrett-Joyner-Halenda (BJH) pore size distribution analyzer assessed the

mesopore size distribution. Surface morphology was analyzed using a Scanning Electron Microscope (SEM). The structural properties were identified using X-Ray Diffraction analyzer and functional groups were examined with a Fourier Transform Infrared spectroscopy (FTIR). Additionally, Energy-Dispersive X-Ray (EDX) Spectroscopy**,** and Thermogravimetric Analyzer (TGA) were employed to evaluate the elemental composition and thermal stability, respectively.

Initially, only BET analysis was performed on all samples to identify which condition yielded the best SSA. Once the best sample was determined, the remaining six characterizations were conducted on that product.

3.6.1. Brunauer-Emmett-Teller (BET) Analysis

The SSA and pore volume of AC were analyzed using a BET analyzer (BELSORP-miniX) through nitrogen (N_2) adsorption-desorption isotherms. A sample weighing 0.0461 grams was measured and degassed to eliminate moisture and other impurities from the surface of the ACs. The amount of nitrogen gas adsorbed was then measured at various relative pressures (P/ P_0), where P represents the pressure and P_0 is the saturation pressure of N_2 gas at 77.35 K. Finally, the SSA was determined.

3.6.2. Barrett-Joyner-Halenda (BJH) Analysis

In the Barrett-Joyner-Halenda (BJH) analysis, the same instrument (BELSORP-miniX), adsorption temperature (77.35 K), and procedure were used as in the BET analysis. However, while the BET analysis focuses on the overall surface area, the BJH analysis specifically examines the distribution of mesopores. Together with this analysis, the N_2 adsorption-desorption was also performed. This was done to validate the BJH pore size distribution and link the surface properties to the adsorption performance.

3.6.3. Scanning Electron Microscope (SEM) Analysis

Scanning electron microscope analysis was performed to study the surface morphology of the ACs (C. Series, 2021). Prior to imaging, the sample were coated for a better image resolution. The analysis was done under high vacuum by applying an accelerating voltage of 5.0 kV.

3.6.4. X-Ray Diffraction (XRD) Analysis

Crystallographic structure and phase composition of the AC produced were identified by X-ray diffraction (XRD). The sample was scanned in 2θ angles to receive the XRD pattern. This method is the analysis of the characteristic peaks of diffraction that allow to know on the one hand the crystallinity of the material and the other the organization of the atomic structure. With regard to carbonaceous materials such as AC, it is especially helpful for determining the difference between the amorphous and crystalline nature and for detecting the existence of the graphitic structure or another crystalline phases.

3.6.5. Fourier Transform Infrared Spectroscopy (FTIR) Analysis

The functional groups on the AC surface were identified by using Fourier Transform Infrared Spectrometer. The spectra were recorded by wave numbers in the range of 400 – 4000 cm^{-1}. Each peak in the spectrum defines a specific functional group.

3.6.6. Energy-Dispersive X-Ray Spectroscopy (EDX) Analysis

Elemental compositions of the fabricated AC were determined using Energy-Dispersive X-ray Spectroscopy. In this analytical technique. The sample is exposed to an intense electron beam, and its constituent elements emit X-rays of characteristic wavelengths. The emitted radiations are then detected using an EDX instrument which offers a precise analysis of atomic number, atomic weight, and percentage content of each element present in the sample. Thus, EDX yields precise information on the purity of the synthesized material and residual constituents. High vacuum in the instrument was used to analyze elemental constituents accurately.

3.6.7. Thermogravimetric Analysis (TGA)

The purity and composition of the AC was investigated through TGA. The analysis took place under an inert atmosphere. The apparatus used was TGA-s 1000 thermogravimetric analyzer. A 3.79 mg sample was measured and heated from room temperature of 27.80 to 798.92°C gradually to examine its thermal profile.

3.7. Experimental Design and Optimization Approach

This study dealt with three independent variables, which are AC dosage, contact time, and mixing speed. The variables were selected based on previous researches (e.g. Arman et al.,

2024; Jumiati, 2024; Miskah et al., 2019; Onn et al., 2023; Sukmawati & Sunarto, 2021; Suryandari & Kusuma, 2021). The major response measured was the percentage removal of FFA as oleic acid.

BBD was employed for the optimization of this response. BBD is a structured statistical method to model complex interactions with a limited number of experimental runs. This design enhances efficiency compared to trial-and-error approaches. Moreover, it helps to identify how different factors interact each other to influence the response.

The design matrix included 17 experimental runs. Among the 17 runs, center points are repeated to estimate experimental error. All experiments were conducted at room temperature. The particle size of the AC was fixed between 100–125 μm. The responses were analyzed using Design-Expert software. In the design expert, ANOVA was conducted to assess the significance of each factor.

This research investigated the interaction between three independent variables. Namely, contact time, AC dosage, and mixing speed. Each variable was assessed at three levels where contact time ranged from 40 to 120 minutes, AC dosage varied from 3% (w/v) to 9% (w/v), and mixing speed was set between 200 and 300 rpm.

Table 3.2: Factors and levels in the BBD for FFA adsorption

Factor	**Symbol**	**Units**	**Levels**		
			Low (-1)	Medium(0)	High(+1)
Contact time	A	Minute	40	80	120
AC Dosage	B	% (w/v)	3	6	9
Mixing Speed	C	Rpm	200	250	300

3.7.1. BBD Matrix for Three Factors

The BBD experimental matrix, that consists 17 experimental runs is presented in Table 3.3.

Table 3.3: Design matrix for FFA removal via BBD

	Factor 1	**Factor 2**	**Factor 3**	**Response 1**
Run	A: Time (min)	B:AC Dosage (% (w/v))	C: Mixing Speed (rpm)	FFA Removal Efficiency (%)
1	120	6	300	*
2	80	6	250	*
3	80	6	250	*
4	120	9	250	*
5	80	6	250	*
6	40	9	250	*
7	80	3	200	*
8	40	6	200	*
9	120	3	250	*
10	80	9	300	*
11	80	9	200	*
12	80	3	300	*
13	80	6	250	*
14	40	3	250	*
15	40	6	300	*
16	80	6	250	*
17	120	6	200	*

A mathematical relationship was established between these factors and the corresponding response, which was the efficiency of FFA removal. The removal efficiency of PET-derived AC in eliminating FFA was evaluated and optimized through 17 experimental runs. The FFA removal efficiency was evaluated for each parameter interaction after conducting two replicates and taking the averages of the results. After the completion of the experimental runs, the data was imported into Design Expert software. Therefore, the significance of the model was

assessed using ANOVA. The ANOVA examined indicators such as the coefficient of determination (R^2 value), probability (p-value), and Fisher values (F-value).

3.8. UCO Treatment

First, a specific amount of AC was weighed using an analytical balance. Next, 50 ml of pretreated UCO was measured and poured into a 200 ml beaker. The UCO sample was then placed on a magnetic stirrer set to a predetermined mixing speed. The adsorbent was gradually added while the UCO was being stirred. After the defined adsorption time, the mixture was filtered to obtain the treated UCO as the filtrate. Analysis of Treated and Untreated UCO.

3.8.1. FFA Determination

This experiment was conducted on both the untreated oil and the 17 treatment variations, as well as for the kinetic study. Average values were calculated for each treatment to ensure precise results. However, the kinetic study was based on a single analysis. Primarily, reagents, including a 0.02 N potassium hydroxide (KOH) solution in ethanol, a 1% phenolphthalein indicator solution, and neutralized 96% ethanol were prepared. The KOH solution was then standardized. Four milliliters of UCO were carefully transferred to a 150 mL Erlenmeyer flask, and the neutralized ethanol was added. The solution was titrated using a burette with the standardized 0.02 N KOH solution. Titration continued until a faint pink color persisted for about 30 seconds, indicating that the endpoint had been reached. The volume of KOH solution consumed was recorded, and the percentage of FFA as oleic acid was calculated using the following formula (Arman et al., 2024).

$$\text{FFA (\% as oleic acid)} = \frac{\text{VxNx28.2}}{\text{W}} \quad \text{..... (3.3)}$$

Where:

V = Volume of the titrant (KOH Solution)

N = Normality of the titrant

W = Weight of sample UCO

3.8.2. PV Determination

The PV analysis is conducted on both untreated UCOs and those treated under optimal conditions. Firstly, reagents were prepared. An acetic acid-chloroform solution (3:2 v/v), a

saturated potassium iodide (KI) solution, a standardized 0.002 N sodium thiosulfate ($Na_2S_2O_3$) solution, and a 1% starch indicator solution was the prepared reagents. Using a micropipette, 4 mL of UCO was carefully transferred to a 150 mL flask. Then, 20 mL of acetic acid-chloroform solution and 0.4 mL of saturated KI solution were added to the oil sample. The mixture was swirled and allowed to react in the dark for 30 minutes. After this period, 20 mL of distilled water and 0.4 mL of starch indicator solution were added. The liberated iodine was immediately titrated with the standardized 0.002 N sodium thiosulfate solution using a burette while stirring vigorously. Titration continued until the blue-black color disappeared. Finally, the volume of sodium thiosulfate solution consumed was recorded, and a blank titration was performed without the oil sample. The PV was then calculated using the formula below (Arman et al., 2024):

$$\mathrm{PV}(\mathrm{meqO_2/kg}) = \frac{(\mathrm{V}-\mathrm{V_0})\mathrm{xNx1000}}{\mathrm{W}} \quad \text{..... (3.4)}$$

Where:

V and V_0 = the volumes (in ml) of $Na_2S_2O_3$ solution and blank, respectively.

N = Normality of the titrant ($Na_2S_2O_3$ solution)

W = Weight of sample UCO

3.8.3. Color Improvement Analysis

Color measurement was performed on both untreated and optimally treated UCOs using a spectrophotometer (CM-600d). Prior to the analysis, the device was calibrated with a standard white tile. Then, the oil samples were placed in a clean, transparent beaker and positioned atop the sensor. The L^* indicate 0 and 100 for darkness and lightness, respectively. The values were recorded at room temperature. And the measurement was duplicated for a better accuracy.

3.9. Optimization of FFA Removal Efficiency

Optimization of operating conditions to remove FFAs from UCO is one of the specific objectives in this study. This objective was achieved by statistical optimization of the experimental results. All variables were systematically varied based on an interaction model predicted by the RSM. Then, their effects on FFA removal were tested. The optimal combinations of operating conditions were determined for maximizing FFA removal efficiency.

3.10. Adsorption Kinetic Study

The kinetic study of adsorption is important to understand the basic mechanisms and rate of adsorption processes (Muhammad et al., 2023). In this study, three kinetic models were used. These were, the PFO, the PSO, and the IPD models. These models were applied to evaluate the adsorption mechanism and rate of FFAs onto the PET-derived AC, X11.

To carry out the kinetic studies, 7.5 grams of AC and 100 ml of pretreated UCO were measured. Then, the mixture was agitated at a speed of 240 rpm for 112 minutes. This was carried out at room temperature. While the agitation continues, samples were taken at constant intervals of 14 minutes. This resulted in nine samples including the zero point. For each sample, a FFA analysis was performed.

Then, the quantity of adsorbed FFA at any time (q_t), was calculated using the following mathematical relation (Wirawan et al., 2022).

$$q_t = \frac{10(FFA_0 - FFA_t) \times m_{uco}}{m_{ac}} \quad \text{..... (3.5)}$$

Where:

q_t = the amount of FFA adsorbed at any time (mg/g)

FFA_0 = the initial FFA percentage as oleic acid (mg/L)

FFA_t = the time-dependent FFA percentage as oleic acid (mg/L)

m_{uco} = the mass of the UCO (g)

m_{ac} = the mass of the AC (g)

3.10.1. PFO Model

According to this model, the rate of occupation of adsorption sites and the number of unoccupied sites are directly proportional (Ho & McKay, 1998). Its applicability usually suggests that physisorption is involved. The linearized equation for this model is given by:

$$\ln(q_e - q_t) = \ln(q_e) - k_1 t \quad \text{..... (3.6)}$$

Where:

t = the adsorption time (min)

q_e= the amount of FFA adsorbed at equilibrium (mg/g)

q_t = the amount of FFA adsorbed at any time (mg/g)

k_1= the rate constant for PFO ($L.\,min^{-1}$)

The values of k_1 and $q_e$can be determined from the slope and intercept of $\ln(q_e - q_t)$ versus t plot, respectively.

3.10.2. PSO Model

The PSO model suggests that the rate of adsorption is proportional to the square of the number of unoccupied sites, implying that chemisorption is the mechanism that controls the rate. The linearized equation for this model is expressed as follows.

$$\frac{t}{q_t} = \frac{1}{q_e}t + \frac{1}{{q_e}^2 k_2} \quad \text{..... (3.7)}$$

Where:

t = the adsorption time (min)

q_e= the amount of FFA adsorbed at equilibrium

q_t = the amount of FFA adsorbed at a time t (mg/g)

k_2= the rate constant for PSO ($g.\,mg^{-1}min^{-1}$)

The values of k_2 and q_e can be calculated from the slope and intercept of the $\frac{t}{q_t}$ versus t linear plot, respectively.

3.10.3. IPD Model

The diffusion model included in the particle indicates where the substance movement through the inner pores of the adsorbent plays some influential part in calculating the overall rate of adsorption. This model is based on the assumption that the adsorption processes involving various steps with some sequential actions needs to be taken into consideration such as in this case the limiting factor is always diffusion. It is given by:

$$q_t = k_i t^{0.5} + C \quad \text{..... (3.8)}$$

Where:

t = the adsorption time (min)

q_t = the amount of FFA adsorbed at a time t (mg/g)

k_i = the rate constant for IPD ($mg.g^{-1}min^{-0.5}$)

4. Results and Discussion

4.1. Yield of PET-Derived AC

The yields of both the char and the ACs are consistent with reported values of previous researches which are in the range of 15 and 30%. Mendoza-Carrasco et al., (2016) found chemical activation with potassium hydroxide achieved yields of 24.62% to 32.07% under controlled heating conditions. The yields reported align with those in this study (Table 4.1). This validates the activation parameters used. Besides, it confirms the production of high-quality AC from PET waste.

Table 4.1: Production Yield of Char and AC for Various Activation Conditions

Sample	Production Yield (%)
C	24.15
D11	23.36
D21	21.67
I11	20.06
I21	18.42
X11	20.83

4.2. Characterization of PET-Derived AC

4.2.1. Brunauer-Emmett-Teller (BET) Analysis

BET analysis was done to determine the SSA. The SSA results from the BET analysis are summarized in Table 4.2.

Table 4.2: BET SSA for a char and AC samples

Sample	SSA (m^2/g)
C	141.9
D11	372.4
D21	742.7
I11	536.5
I21	724.1
X11	984.9

The results of this study showed the optimal methods and conditions to produce AC. Based on this analysis, X11 was selected due to its larger SSA) compared to the other four ACs. Therefore, this finding indicates that double activation is the most effective approach.

After selecting X11, further analysis of its BET results was conducted. The reliability of the measured SSA is highly supported by the statistical fit of the experimental data to the BET equation. The analysis resulted a high correlation coefficient (R^2) of 0.9998, which indicates an excellent linear relationship. Because of this R^2 value, the accuracy of the result is found to be valid. Moreover, the BET constant, C was measured to be 600.35. And a C value significantly greater than 200 is characteristics of microporous materials and high affinity of the AC surface (Thommes et al., 2015).

The nitrogen adsorption-desorption isotherm shows that the AC X11 consists primarily of micropores. However, as illustrated in Figure 4.1, it shows a type IV pattern, which is characterized by an H4-type hysteresis loop between relative pressures of 0.4 and 0.9. The loop suggests the presence of mesopores, even if micropore structures outnumber (Thommes et al., 2015).

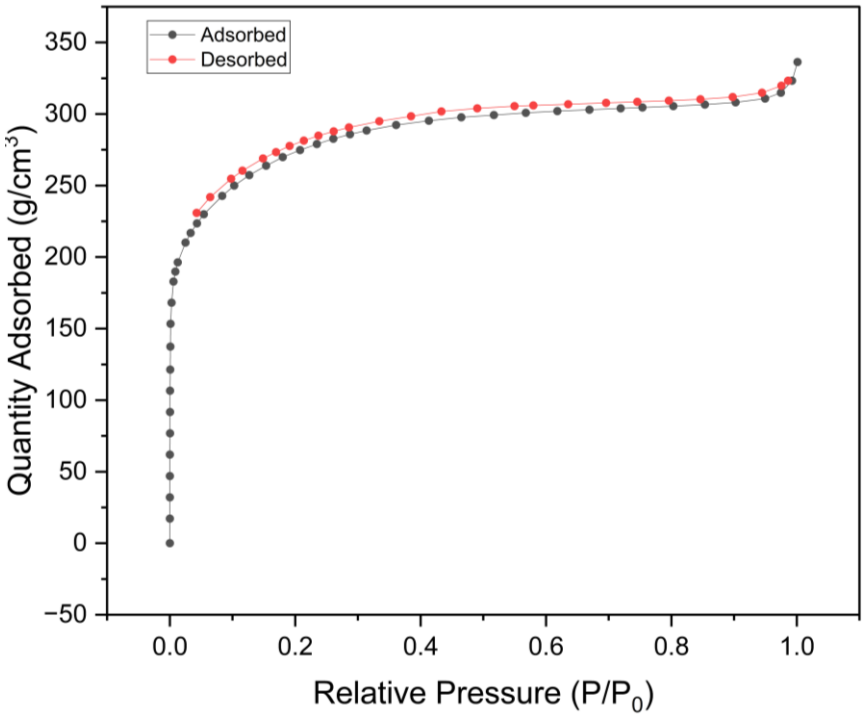

Figure 4.1: N_2 Adsorption-Desorption Isotherm

4.2.2. Barrett-Joyner-Halenda (BJH) Analysis

Figure 4.2 shows the BJH plot for X11, which indicates that it is a mesoporous material. The average pore diameter and the total pole volume were identified to be 2.024 nm and 0.498 cm^3/g. These results indicate a structure predominantly composed of narrow mesopores. According to IUPAC standards, Adsorbent pore sizes are categorized into three primary types. These are micropores (pore diameters less than 2 nm), mesopores (pore diameters ranging from 2 to 50 nm), and macropores (pore diameters greater than 50 nm) (Thommes et al., 2015). Therefore, the average pore diameter of 2.0238 nm indicates that the AC X11 consists of narrow mesopores.

The nitrogen adsorption-desorption isotherm (from BET analysis) of X11 agrees with the findings from the BJH analysis. This interpretation is consistent with BJH analysis, which demonstrates narrow mesopore presence. Such kind of pore arrangement enhances mass transfer and ideal for medium-size organic molecules like FFAs (Rezki et al., 2020). Moreover, according to Virtanen et al., (2020) ACs with narrow mesoporosity exhibit both high adsorption capacity, and improved regeneration performance in oil purification.

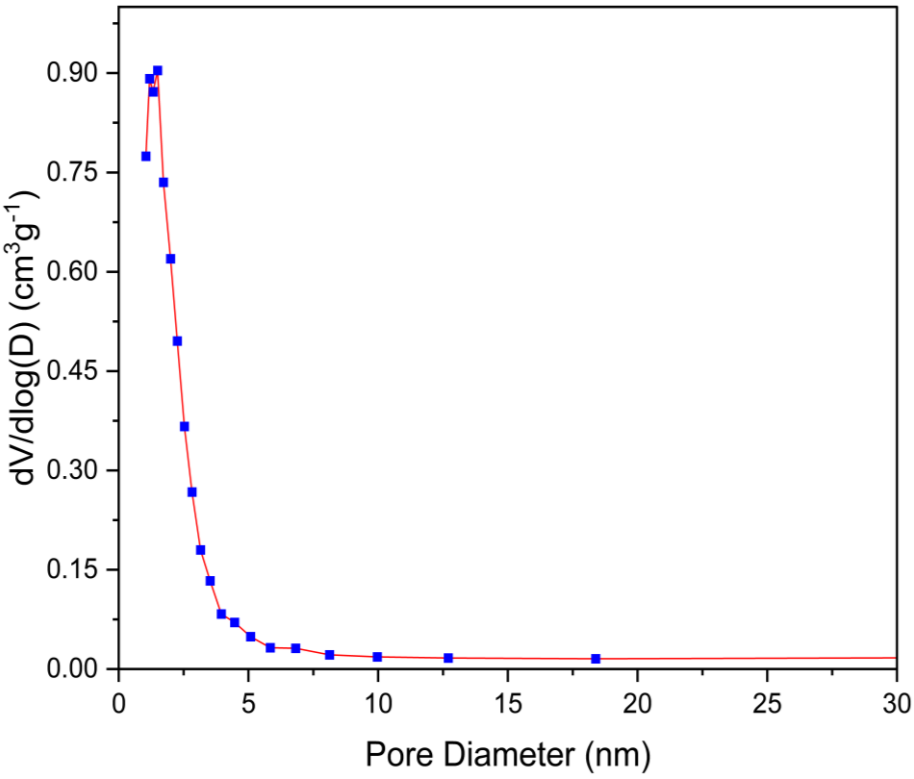

Figure 4.2: Pore size distribution for X11

4.2.3. Scanning Electron Microscope (SEM) Analysis

Figure 4.3 presents the SEM image of the surface morphology of X11. Image (a) shows the surface of the prepared sample was cavities and interconnected pores. By a higher magnification of (image (b)), the surface exhibits finer detail with many smaller holes in the larger pores as well as evidence of particle interconnection. Image (c) reveals a similar behavior, where a dense spongy structure of fine pores associated with large agglomerated particles are shown. Finally, Image (d) shows widespread agglomeration with well-formed interconnected pores. Summary SEM images demonstrate that X11 can be used for the physical and chemical bonding interactions.

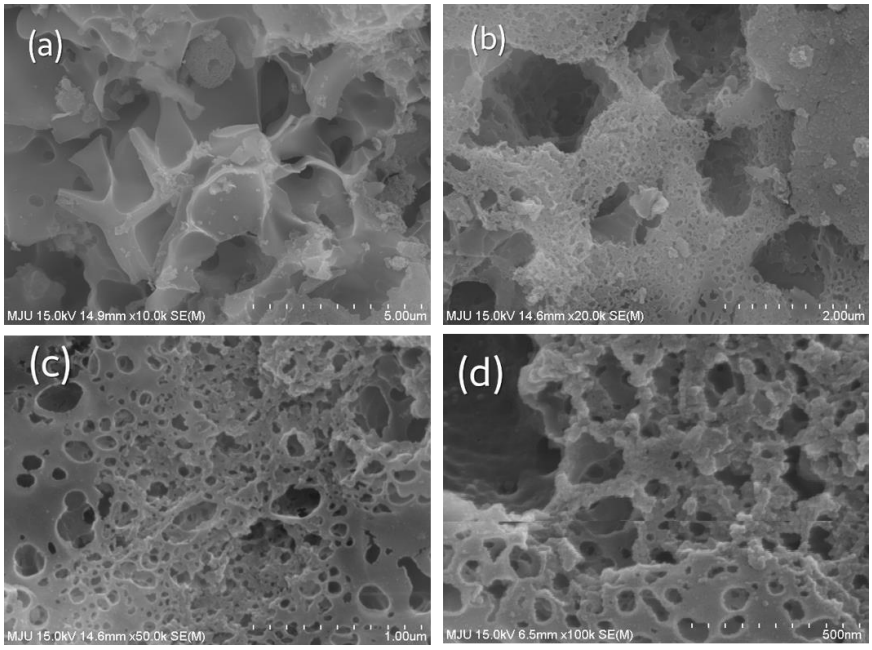

Figure 4.3: SEM images for X11 at resolution of (a) 10k, (b) 20k, (c) 50k, and (d) 100k

4.2.4. X-Ray Diffraction (XRD) Analysis

The XRD pattern presented in Figure 4.4 provides important insights into the structural properties of the material. As shown, there is a broad peak observed between 15° and 30° 2θ around a high intensity between 22-24°, which is characteristic of lowly graphitized carbonaceous materials with amorphous and semi-crystalline features. This characteristic of the ACs in their normal formation has been described as the (002) diffraction peak. The peak discovered the presence of disordered graphitic layers with limited long range order (Pham, 2023; Shahcheragh et al., 2023). The absence of prominent, sharp peaks, which can be clearly defined in the presented patterns, suggests the absence of highly crystalline phases. This fact

correlates with the material being AC, which is usually synthesized utilizing operations that destroy orderly arrangements in order to produce a porous structure. This amorphous structure is essential for the material's high surface area, which is critical for most of its applications, specifically, adsorption (Abdul Khalil et al., 2013; Yuan et al., 2020). The lack of obvious distinct peaks throughout the whole 2θ range also confirms that the material is primarily amorphous.

Shahcheragh et al. (2023) reported that activated carbon derived from almond shells and palm kernels displayed a broad peak at low diffraction angles. This peak indicates the presence of disordered graphitic layers with very small crystallite domains, a characteristic feature of amorphous activated carbons. At higher 2θ values, some very weak intensity fluctuations can be seen which could be related to minor and less ordered crystalline phases. However, no distinct peaks at any angle are visible here. This weak intensity ranging is most likely either very small regions of crystal of an overall amorphous particle, or they are present in an overall quantity which is not enough to produce visible diffraction. Thus, the XRD profile most certainly confirms the formation of an AC with very high disorder quite successfully.

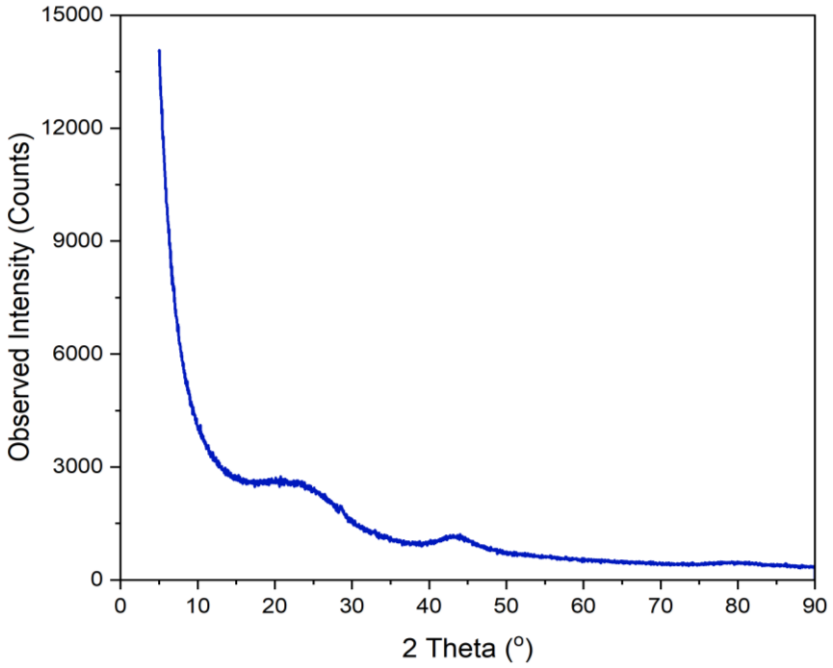

Figure 4.4: XRD pattern of X11

4.2.5. Fourier Transform Infrared Spectroscopy (FTIR) Analysis

A number of functional groups are depicted on Figure 4.5 which may be found in the AC X11 surface chemistry. A broad absorption band is identified in the range of 3000 to 3650 cm^{-1} with

a weak transmittance minimum at 3429 cm^{-1}. This strong and broad band is related to the stretching vibrations of the hydroxyl (-OH) group (Nandiyanto et al., 2023). The strength, black width of the band is a clear sign of the presence of a large number of oxygen-containing functional groups, which are directly involved in the adsorption of polar species. Since FFAs possess a polar carboxylic acid (-COOH) group, FFAs provided strong hydrogen bond adsorption by surface hydroxyls (Onn et al., 2023). Peroxides, high polarity, and hydro peroxide (-OOH) linkages are also effectively adsorbed in a similar fashion through hydrogen bonding mechanisms (Francisco & Villalobos, 2024).

The presence of 2365 cm^{-1} also indicates adsorption of CO_2 confirming the interaction between carbon and CO_2 (Yahia et al., 2024). Another important interaction characteristic is in the range of 1500 to 1700 cm^{-1} with its peak at 1635 cm^{-1}. This is likely due to C=C stretching vibrations in the carbon material's aromatic carbon framework (Nandiyanto et al., 2023). The appearance of this functional group is significant for physical adsorption. In addition, in the range of 1000 to 1400 cm^{-1}, the peak at 1046 cm^{-1} and 1385 cm^{-1} have been observed. The bands are typical for C-O stretching vibrations, and the presence of several functional groups of oxygen on the surface of X11 is observed (Nandiyanto et al., 2023; Suryandari & Kusuma, 2021).

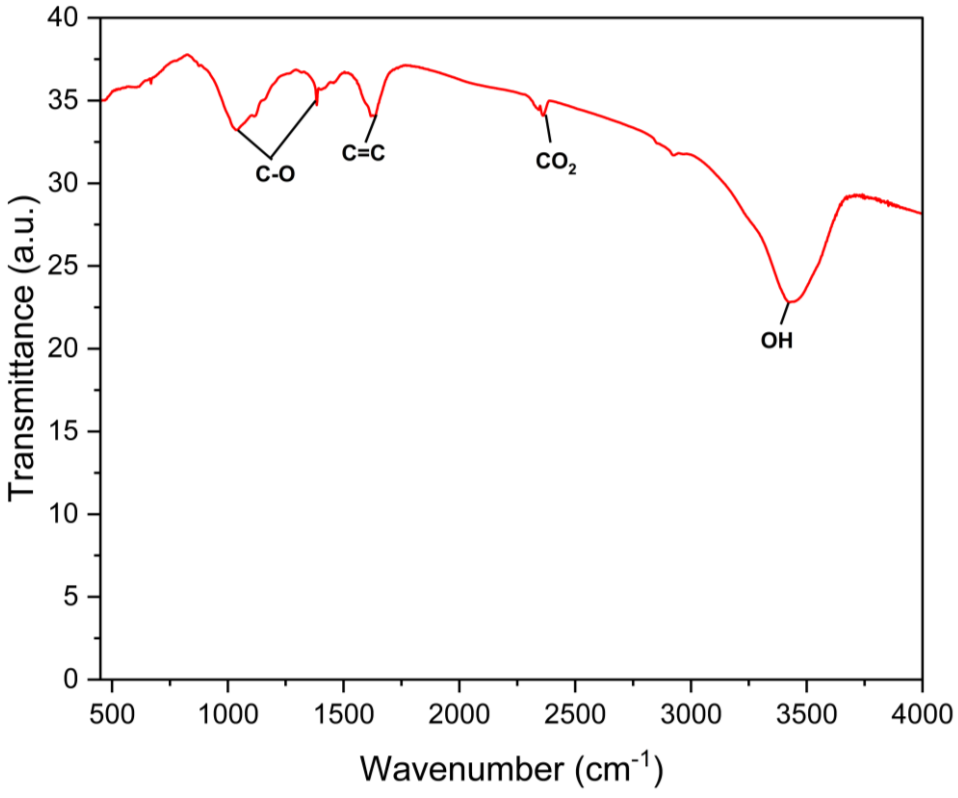

Figure 4.5: FTIR spectrum of X11

4.2.6. Energy-Dispersive X-Ray Spectroscopy (EDX) Analysis

In order to fully characterize the material's elemental composition, Energy Dispersive X-ray analysis was also performed. The following list includes both quantitative outcomes and the representative spectrum. The inset table in Figure 4.6 shows the atomic and weight percentages of the detected elements, while the figure depicts the EDX-spectrum. The latter demonstrates the characteristic X-ray emission peaks.

The outcomes of this analysis indicate that the material mostly consists of carbon and oxygen with atomic percentages of 50.02% and 30.99%, respectively. The fact that the high concentration of carbon and oxygen is proved to be the redeeming element confirms the anticipated composition. Instead, AC is defined as a carbonaceous material where surface oxidation occurs through the activation process. In addition, the EDX spectrum presents a graphical confirmation of these outcomes since a high peak of carbon at approximately 0.277 keV and oxygen at nearly 0.525 keV is observed. In addition, the corresponding peak for potassium at approximately 3.314 keV, and aluminum at roughly 1.486 keV, which are presented at a lower intensity compared to carbon and oxygen.

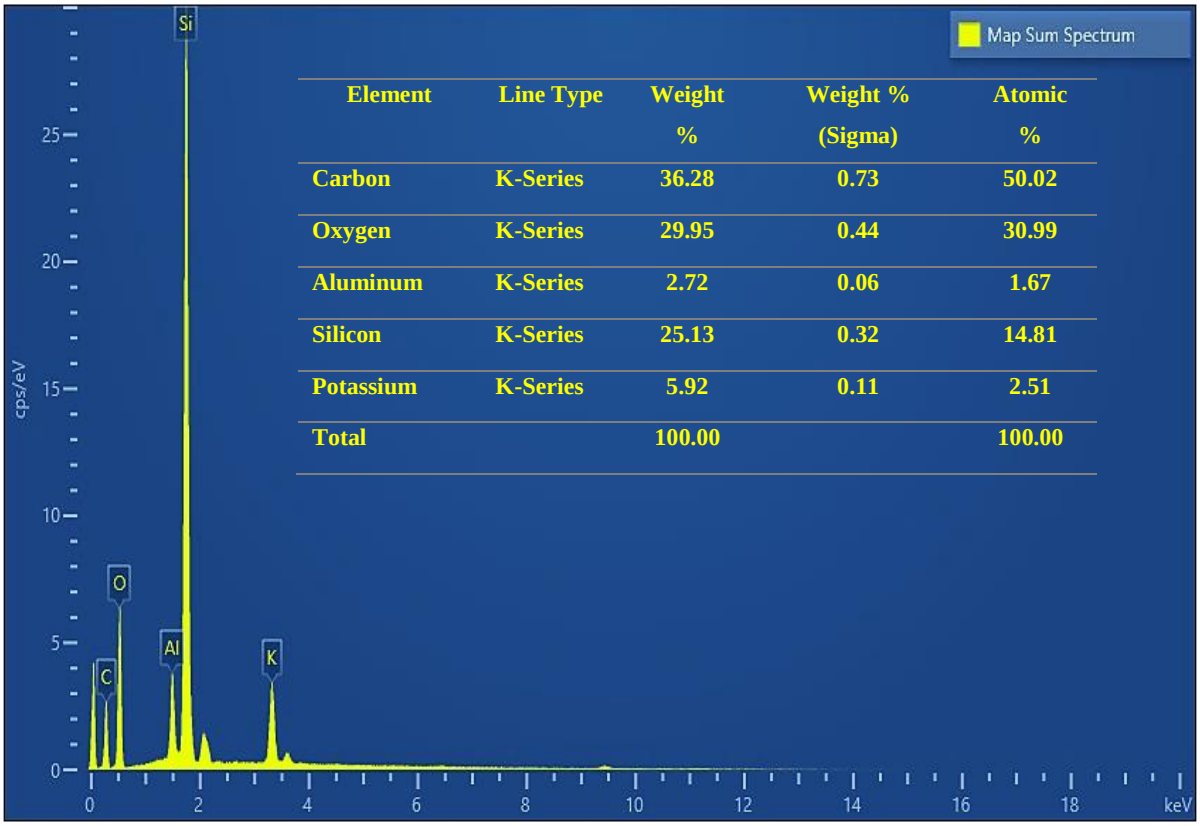

Element	Line Type	Weight %	Weight % (Sigma)	Atomic %
Carbon	K-Series	36.28	0.73	50.02
Oxygen	K-Series	29.95	0.44	30.99
Aluminum	K-Series	2.72	0.06	1.67
Silicon	K-Series	25.13	0.32	14.81
Potassium	K-Series	5.92	0.11	2.51
Total		100.00		100.00

Figure 4.6: EDX elemental analysis of X11

4.2.7. Thermogravimetric Analysis (TGA)

The thermogravimetric analysis reveals a multistage thermal decomposition process. The analysis was done for assessing the purity and composition of the AC sample. An initial mass reduction of approximately 2.77% was observed in the lower temperature range from ambient temperature (27.8°C) up to 150°C. This primary decrease in mass is attributed to the desorption of physically adsorbed moisture, a common occurrence in porous carbonaceous materials (Alabi-Babalola et al., 2024; De Castro et al., 2018). Following this initial dehydration phase, a more significant weight loss occurs, indicating thermal decomposition of specific surface functional groups. In this phase, between 150°C and 450°C, the weight loss was about 5.4%. This segment of the curve is characteristically associated with the evolution of less stable oxygen-containing moieties, such as carboxylic acids and lactones, which are commonly found on the surfaces of ACs and significantly contribute to their chemical reactivity (Salgado et al., 2018).

As the thermal process continues from 450°C to the last recorded temperature 796°C, a constant weight loss could be still observed, amounting to 2.7%. This degradation in general is believed to occur on the higher thermally stable oxygen functional groups, such as phenolic and ethereal group. In addition, an incremental thermal remodeling of the core carbon skeleton is happening itself (Salgado et al., 2018). The total weight loss of 10.87% suggests the existence of volatile content and different functional groups on the surface of the AC sample. This study and other instance of characterization evaluate the potential of X11 for special applications, such as UCO treatment.

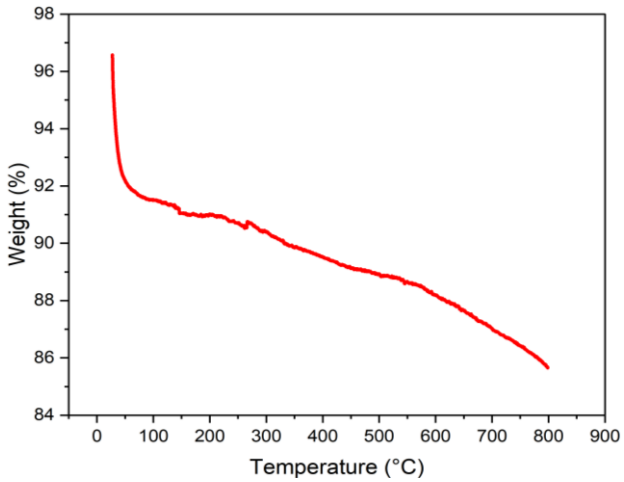

Figure 4.7: TGA curve of X11

4.3. Physicochemical Characteristics of UCO Prior to Treatment

The untreated UCO was characterized before carrying out the adsorption operation. The FFA as oleic acid, the PV, and the color lightness were measured before the treatment. Table 4.3 summarizes the characterization results.

Table 4.3: UCO characterization results before adsorption treatment

Characteristics	Values
FFA (% oleic acid)	1.2860
PV (mgO_2/kg)	29.3100
Color lightness (L^*)	25.1700

4.4. BBD and Model Prediction

Table 4.4 summarizes the experimental runs from the Box-Behnken Design (BBD) that investigated the effects of contact time, activated carbon (AC) dosage, and mixing speed on free fatty acid (FFA) removal efficiency. The data reveal clear trends regarding these key factors.

Contact time significantly affects FFA removal, with longer durations generally resulting in higher efficiencies. For instance, runs conducted for 120 minutes, such as Run 4 with a 9% AC dosage, achieved removal efficiencies exceeding 67%. In contrast, shorter durations, like 40 minutes, yielded considerably lower removal rates, sometimes falling below 30%.

AC dosage also plays a crucial role; increasing the dosage enhances removal due to a greater number of available adsorption sites. High dosages (9%) consistently produced better removal outcomes, as demonstrated in Runs 4 and 11, compared to lower dosages (3%), which resulted in removal efficiencies as low as 27% in Run 14.

The effect of mixing speed is more complex. While effective stirring is essential for optimal contact and mass transfer, the data do not indicate a straightforward positive correlation between higher rpm and removal efficiency. Some runs at moderate mixing speeds (200-250 rpm) achieved better results than those at 300 rpm, suggesting that mixing speed interacts with time and dosage to influence the outcome.

Overall, the highest FFA removal efficiencies were observed with longer contact times and higher AC doses, while the influence of mixing speed depends on its interaction with the other

factors. This dataset underscores the importance of optimizing all three parameters to enhance adsorption performance.

Table 4.4: BBD experimental runs with factor levels and response data

Order	**Factors**			**Response**
Run	Time (min)	AC Dosage (% (w/v))	Mixing Speed (rpm)	FFA Removal Efficiency (%) Actual
1	120	6	300	60.80
2	80	6	250	61.40
3	80	6	250	60.80
4	120	9	250	67.50
5	80	6	250	60.80
6	40	9	250	46.30
7	80	3	200	46.40
8	40	6	200	44.60
9	120	3	250	48.80
10	80	9	300	57.80
11	80	9	200	63.80
12	80	3	300	42.10
13	80	6	250	62.70
14	40	3	250	27.10
15	40	6	300	43.40
16	80	6	250	62.10
17	120	6	200	64.30

4.5. Statistical Analysis for FFA Removal

4.5.1. Sequential Model Sum of Squares

The FFA removal efficiency was evaluated by the Sequential Model sum of Squares (Type I). The straight-line term was found to explain the much of the variation in response and was highly significant ($p = 0.0003$). Sensitivity testing for the incorporation of 2FI terms after the linear term was found not to add significantly (p-value = 0.9974). However, a notable

enhancement in the model's fit was observed with the inclusion of a quadratic term. This addition proved highly significant, indicated by a p-value of less than 0.0001 and a substantial F-value of 79.44. This suggested a strong non-linear relationship was present. A cubic term was tested as well, but it was not statistically significant (p = 0.0706) and more importantly, as "Aliased," indicating that the model could not be used for the particular model. Therefore, in terms of statistical significance and lack of aliasing, the quadratic model was selected as the best representation of the FFA removal efficiency.

Table 4.5: Sequential model of sum of squares for response model selection

Source	Sum of Squares	Df	Mean Square	F-value	p-value	
Mean vs Total	49864.03	1	49864.03			
Linear vs Mean	1458.25	3	486.08	13.03	0.0003	
2FI vs Linear	2.11	3	0.7025	0.0145	0.9974	
Quadratic vs 2FI	**469.07**	**3**	**156.36**	**79.44**	**< 0.0001**	**Suggested**
Cubic vs Quad.	11.01	3	3.67	5.29	0.0706	Aliased
Residual	2.77	4	0.6930			
Total	51807.23	17	3047.48			

4.5.2. ANOVA

An ANOVA was performed on the quadratic model for FFA removal efficiency. The overall model had p-value < 0.0001 and F-value = 108.93). The model's F-value of 108.93 implies the model is significant. There is only a 0.01% chance that an F-value this large could occur due to noise. Additionally, the lack of fit for this model was non-significant (p = 0.0706). This confirms the validity of the quadratic model in interpreting the experimental data.

In terms of individual factors, A-Time (p < 0.0001), B-AC Dosage (p < 0.0001), and C-Mixing Speed (p = 0.0069) were identified as significant contributors to FFA removal efficiency since the p-values are less than 0.05. In contrast, the two-factor interaction terms AB (p = 0.8636), AC (p = 0.4394), and BC (p = 0.5637) were not statistically significant. This suggests that interactions between these pairs of factors did not have a meaningful impact. The quadratic terms A-Time squared (A^2, p < 0.0001) and B-AC Dosage squared (B^2, p < 0.0001) were also significant, which indicates a curvilinear relationship for these factors. But, the quadratic term

for C-Mixing Speed (C^2) had a p-value of 0.0527, which indicates that it did not reach significance at $p < 0.05$.

Overall, this ANOVA insisted that the quadratic model is a robust and suitable fit for the FFA removal efficiency data. This clearly highlights the significant main and curvilinear effects of the experimental parameters studied. Table 4.6 presents the ANOVA for the selected quadratic model.

Table 4.6:ANOVA for the quadratic model fitted to the experimental data

Source	Sum of Squares	Df	Mean Square	F-value	p-value	
Model	**1929.42**	**9**	**214.38**	**108.93**	**< 0.0001**	**Significant**
A-Time	800.00	1	800.00	406.47	< 0.0001	
B-AC Dosage	630.13	1	630.13	320.16	< 0.0001	
C-Mixing Speed	28.13	1	28.13	14.29	0.0069	
AB	0.0625	1	0.0625	0.0318	0.8636	
AC	1.32	1	1.32	0.6720	0.4394	
BC	0.7225	1	0.7225	0.3671	0.5637	
A^2	188.59	1	188.59	95.82	< 0.0001	
B^2	233.22	1	233.22	118.50	< 0.0001	
C^2	10.68	1	10.68	5.43	0.0527	
Residual	13.78	7	1.97			
Lack of Fit	**11.01**	**3**	**3.67**	**5.29**	**0.0706**	**not significant**
Pure Error	2.77	4	0.6930			
Cor Total	1943.20	16				

4.5.3. Fit Statistics

Fit statistics were used to evaluate the overall quality and reliability of the model. An observed high R^2 value of 0.9929 indicates that approximately 99.3% of the variation in FFA removal efficiency could be explained by the model. This strong explanatory power was further supported by an Adjusted R^2 of 0.9838, which accounts for the number of terms in the model and remains very high. Additionally, the model demonstrated predictive power with a predicted R^2 value of 0.9072. The predicted R^2 showed reasonable agreement with the Adjusted R^2, as their difference was less than 0.2, which is typically regarded as a positive indicator of model robustness.

The Adequate Precision, an important measure of the signal-to-noise ratio and model quality, was 35.0843. The ratio significantly exceeds the acceptable ratio of 4. This indicates that a satisfactory signal can be obtained, validating the model's suitability for exploring the design space. Other measures, such as a standard deviation of 1.40 and a coefficient of variation (C.V. %) of 2.59, were also observed. Together, these fit statistics provide strong evidence for an excellent model fit, good predictive capability, and overall reliability in representing the FFA removal efficiency data.

Table 4.7:Fit summary for the developed model

Std. Dev.	1.40	R^2	0.9929
Mean	54.16	Adjusted R^2	0.9838
C.V. %	2.59	Predicted R^2	0.9072
		Adequate Precision	35.0843

4.5.4. Diagnostic Plots

For assessing the accuracy of the developed model, two diagnostic plots, that correspond to the most important regression assumptions were chosen. The plots are ideal for the demonstration of the model's reliability.

4.5.4.1. Normal Probability Plot of Residuals

Normal plot of residuals was done to assess the model assumption. This plot provides a visual examination of whether the residuals (i.e., differences between observed and predicted values) is normally distributed. The best fit for the data points is a straight line that diagonally crosses the plot. A perfect line indicates that the residuals of the model are normally distributed, which is a fundamental assumption for many statistical tests, including ANOVA. From the plot in Figure 4.8, the data points were observed to be relatively close to the straight line. Therefore, it suggested the residuals to be normally distributed. This visual fit validates the model formulation and the subsequent analyses made with the model.

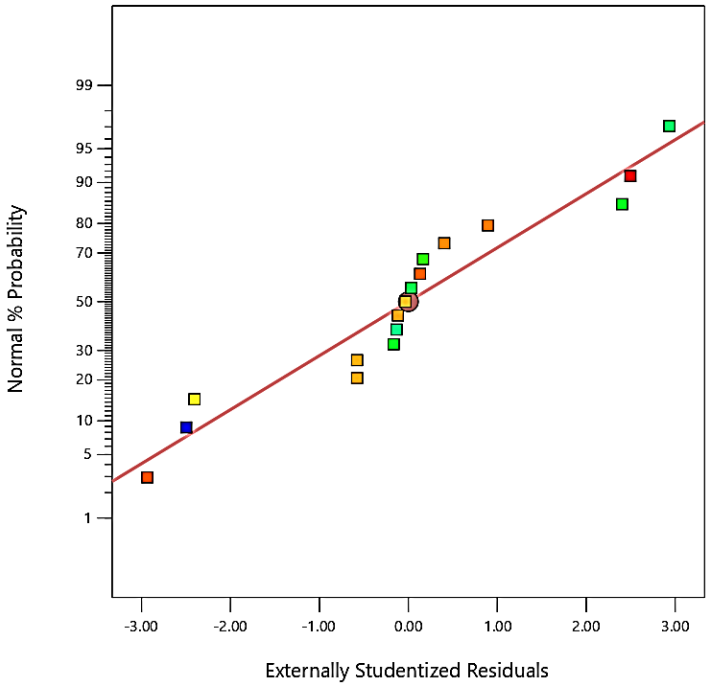

Figure 4.8: Normal probability plot of residuals for FFA removal efficiency

4.5.4.2. Predicted Values Vs Actual Values Plot

The performance of the model was also assessed visually using the Predicted versus Actual plot shown in the Figure 4.9. This plot is a very simple way of showing how closely the predictions of the model matched up to what was actually observed during the experiments. In principle, if the model was perfect, all of the data points would be located on the 45-degree line, which is perfectly aligned with predicted value equaling actual value.

For the plot that resulted from this study, the majority of the data points were seen to be very close to the ideal, straight-line relationship. The validity of the predicted values was found to be very closely aligned to the actual FFA Removal Efficiency as measured during the experiments. The scatter of data points around the dashed line appeared fairly consistent again confirming some reliability to the model along the available range of FFA removal efficiencies. Overall evidence was very promising; a developed model with good predictive capabilities, and reliable estimation capacity for FFA Removal Efficiency given the conditions of this study.

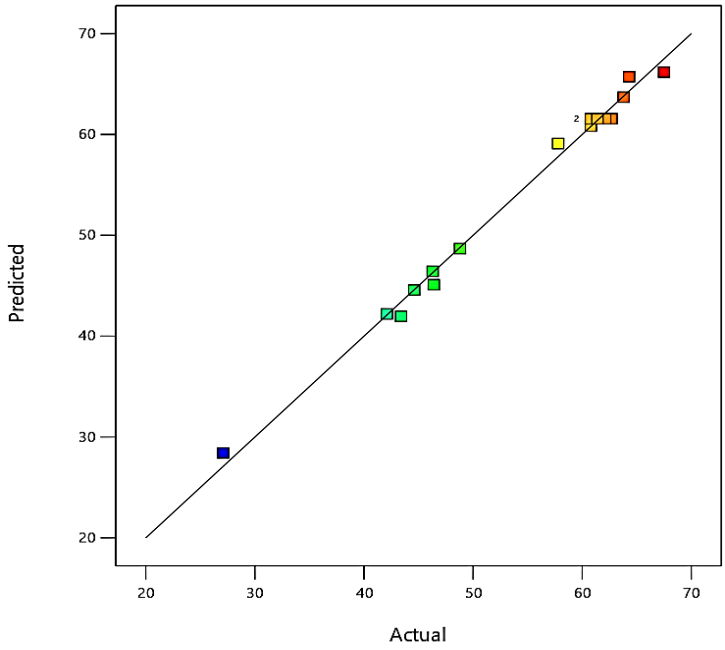

Figure 4.9: Actual vs predicted values for FFA removal efficiency

4.5.5. Combined Effects of the Independent Variables

The complex associations among the different experimental factors and FFA removal efficiency were shown using a set of three-dimensional (3D) response surface plots as put in Figure 4.10. Response surface plots are unique features of RSM, and they perform the function of demonstrating how two factors change while a third factor is held constant and how all three factors influence the response, including the identification of maximum or minimum operating conditions.

The first 3D surface plot (a) depicts the FFA removal efficiency as affected by A: time (min) and B: AC dosage (% (w/v)), while holding factor C: mixing speed constant at 250 rpm. The surface exhibited a prominent peak, signifying an optimal relationship between the two factors. The Points on the surface plot peaked at the upper limits of both time (around 120 min) and AC dosage (around 9% (w/v)), highlighted by the dark red and orange regions. This strongly indicated that increasing both reaction time and AC dosage (within the studied limits) would produce the greatest FFA removal efficiency, while keeping mixing speed constant.

The second plot (b) demonstrates FFA removal efficiency against A: time (min) and C: mixing speed (rpm), with factor B: AC dosage held constant at a 6% (w/v) level. This surface also had distinct curvature. FFA removal efficiency mostly increased with time, but the steepest increase occurred relatively early in the process and likely because of the reaction mechanism/phases,

before improving again less steeply at longer times. Also confirming visually with the gradient of colors on the surface that the FFA removal efficiencies were greatest. Approximately 67.5% were those achieved with longer times in combination with intermediate mixing speeds.

Last, the third surface plot was (c) the representation of the FFA removal efficiency along B: AC dosage (% (w/v)) and C: mixing speed (rpm), keeping fixed the factor A: time at 80 min. With respect to mixing speed, the performance tended to going to a plateau (or a weak peak) near mid-values, indicating that very high/low mixing speeds might not be always optimal. Surface contours with different ranges of color, from blue (less efficient) to red (more efficient), also visually confirmed that the best FFA removal (up to 67.5%) was achieved at higher AC dosages associated with a middle mixing speed.

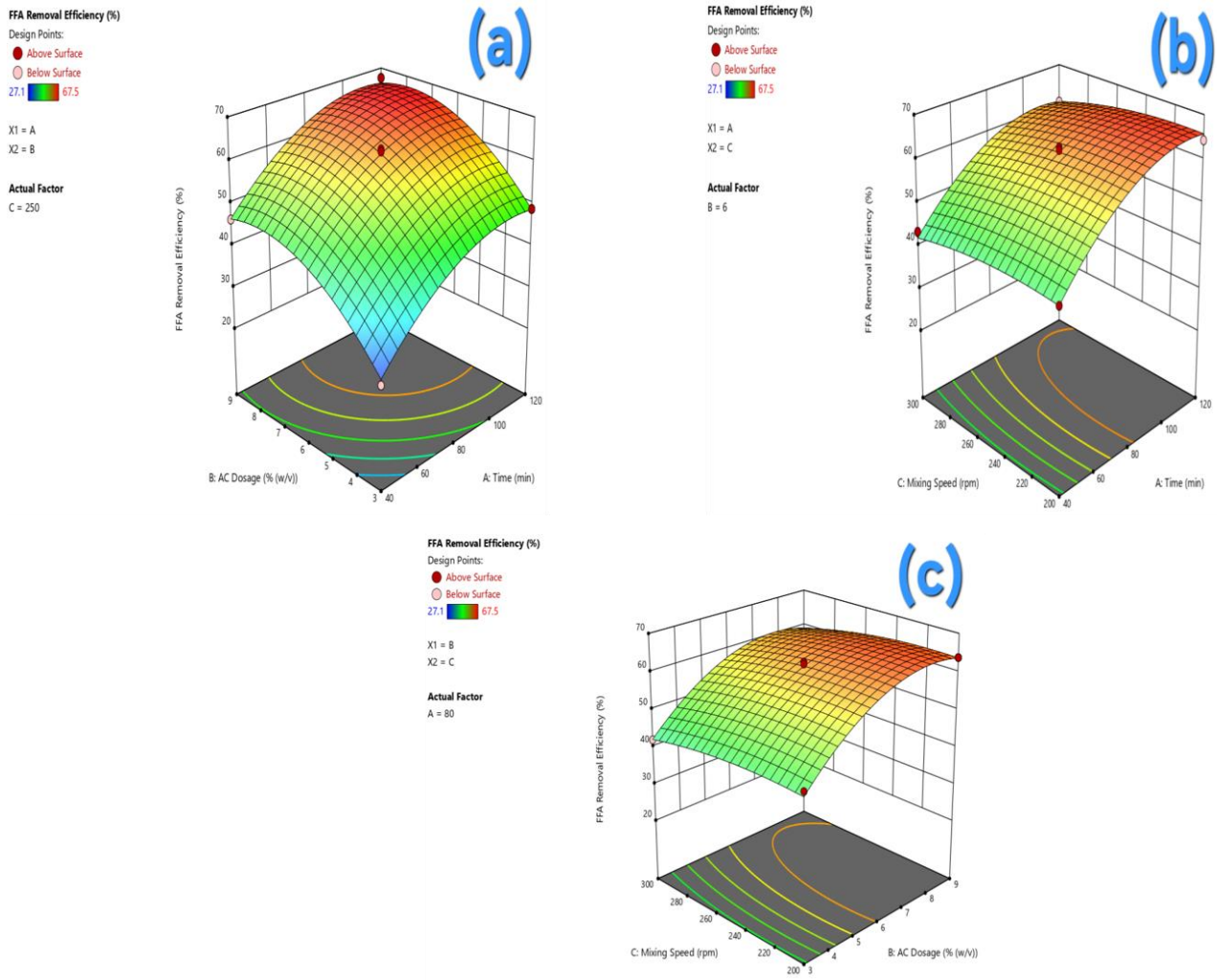

Figure 4.10: 3D surface plots for combined effects of factors on FFA removal efficiency: (a) time and AC dosage, (b) mixing speed and time, and (c) mixing speed and AC dosage

4.5.6. Statistical Optimization of Independent Variables

Understanding the influence of single effects on FFA removal efficiency is generally complemented by the knowledge of combined effects, in particular of interaction effects. Although particular interactions may not show statistical significance, the general response surface also shows a complicated interaction and a non-uniform response pattern for simultaneous adjustment of various factors, as observed in the 3D plots. And, it is just this complex dynamic character of the response surface that demands some systematic optimization. The objective of the statistical optimization was to carefully determine the best combination of the independent variables (time, AC dose and mixing speed), which could lead to the maximum FFA removal efficiency from the experimental design space as possible.

Table 4.8: Optimization criteria for factors and response

Factor/Response	Goal	Lower Limit	Upper Limit
A:Time	is in range	40	120
B:AC Dosage	is in range	3	9
C:Mixing Speed	is in range	200	300
FFA Removal Efficiency	maximize	27.1	67.5

Based on the optimization process, a specific set of optimal conditions was identified. These are a time of 111.55 minutes, a mixing speed of 236.21 rpm, and an AC dosage of 7.49% (w/v). Under these conditions, the model predicted a FFA removal efficiency of 68.41%. To validate this prediction, two confirmatory experiments were conducted. The individual experimental results for FFA Removal Efficiency were recorded as 67.86% and 68.54%. The average of these two experimental runs was determined to be 68.20% removal efficiency. A close agreement was observed between the predicted and experimentally verified removal efficiencies; specifically, the absolute difference was 0.27 percentage points only. This excellent agreement validated the model's predictive capability.

Table 4.9: Predicted and observed values of factors and response in the optimization experiment

Factors	Contact Time (min)	AC Dosage (%(w/v))	Mixing Speed (rpm)	FFA removal efficiency (%)
Predicted	111.72	7.49	236.21	68.41
Observed (1)	112.00	7.50	240.00	67.82
Observed (2)	112.00	7.50	240.00	68.54
Observed (Average)	112.00	7.50	240.00	68.20
Remark: PET-based AC showed superior adsorption performance compared to bio-mass based ACs.				

4.6. Kinetic Studies of FFA Adsorption

Rate and mechanism of adsorption were studied through kinetic studies. Having this knowledge is important to explain the process scientifically (Nayak et al., 2017). Therefore, in this study, the three common models, PFO, PSO, and IPD were applied.

The experimental data used for the kinetic study is presented in the Table 4.10 below.

Table 4.10: Kinetic studies experimental data

Time (minutes)	FFA removal efficiency (%)
0	0.00
14	20.30
28	36.21
42	49.03
56	59.18
70	62.44
84	62.76
98	64.53
112	64.86

The corresponding experimental adsorption kinetics curve is shown in the figure 4.11. The graph shows that the adsorption rate is fast at the beginning of the process. Then, after t = 70 minutes the rate becomes very slow and approaches an equilibrium state.

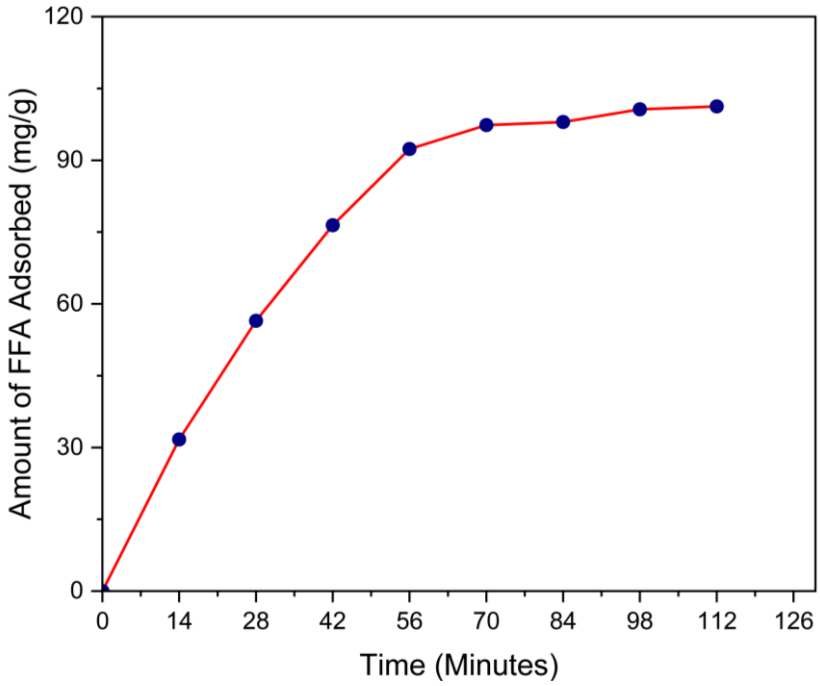

Figure 4.11: Experimental adsorption kinetics curve

As shown in the Figure 4.12 (a) below, the kinetic data points of the PFO model show a strong linearity. The regression analysis yielded an R^2 value of 0.9644. The calculated PFO rate constant (k_1) and equilibrium capacity ($q_{e,calc}$) were 0.0504 min^{-1} and 146.29 mg/g, respectively.

PSO model was also applied to the kinetic data. In its graph (Figure 4.12, b), the linear relationship is clearly visible for the data. The linear regression analysis results an R^2 value of 0.9657, which is slightly higher than for the PFO model. The PSO adsorption rate constant (k_2) was determined to be 0.000166 $g.mg^{-1}.min^{-1}$ while the equilibrium adsorption capacity ($q_{e,calc}$) was calculated to be 144.93 mg/g.

Additionally, IPD was applied to assess the contribution of diffusion in the adsorption process. As depicted in Figure 4.12 (c), the kinetic data results a good linear relationship with an R^2 of 0.9522. From this model, the IPD rate constant (k_i) was obtained to be 10.504 $mg.g^{-1}min^{-0.5}$ and the intercept (c) was 1.48 mg/g.

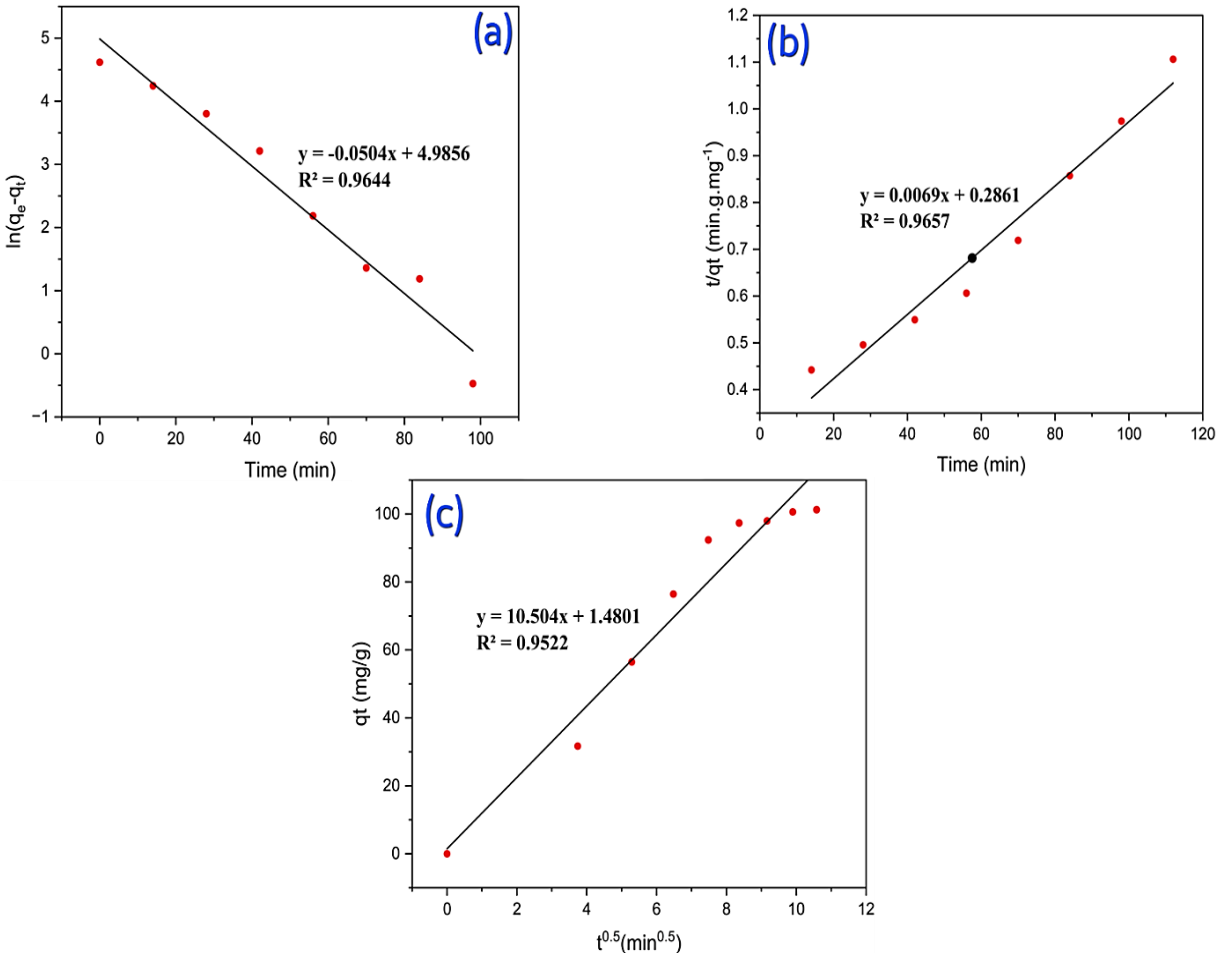

Figure 4.12:Plots of kinetic studies for the adsorption of FFA: (a) PFO, (b) PSO, and (c) IPD

Table 4.11 summarizes the findings from all investigated models, showing high R^2 values across the board. However, a significant difference exists between the experimental and calculated equilibrium adsorption capacities in the PFO and PSO models. This suggests that these models do not fully capture the adsorption process, particularly its ultimate capacity. Nevertheless, the higher R^2 value for the PSO model indicates that the chemical interaction between FFAs and the adsorbent is the dominant factor, although this does not imply that only chemisorption occurs. According to Zhang et al., (2024), the similarity in R^2 values may suggest that both physisorption and chemisorption are involved, likely due to the high porosity of the adsorbent used. Similar findings were reported by Jamal & Boulanger, (2010) and Ilgen & Dulger, (2016), who also observed close and identical R^2 values. Additionally, the analysis of IPD indicates that this factor also contributes to the adsorption process.

In conclusion, the adsorption of FFAs onto PET-derived AC involves both surface reaction processes and mass transfer. This indicates that the process has a complex reaction mechanism. The PSO model more accurately represents the reaction rate than the PFO model, while the

IPD model determines the diffusion rate. Therefore, k_2 and k_i these are the rate-determining constants.

Table 4.11: Summary of kinetic model parameters of FFA adsorption

Kinetic Model	Parameters	Value
PFO	$k_1 x10^2 (min^{-1})$	5.0400
	$q_{e,exp}$ (mg/g)	101.2600
	$q_{e,calc}$ (mg/g)	146.2900
	R^2	0.9644
PSO	$k_2 x10^4$ ($g.mg^{-1}.min^{-1}$)	1.6666
	$q_{e,exp}$ (mg/g)	101.2600
	$q_{e,calc}$ (mg/g)	144.9300
	R^2	0.9657
IPD	k_i ($mg.g^{-1}min^{-0.5}$)	10.5040
	C (mg/g)	1.4800
	R^2	0.9522

4.7. Removal of Additional Impurities under Optimized Conditions

Oil quality is more than just FFA content. Oxidation products, color, and odors also play a huge role. The PV measures oxidation while color and odor are crucial aesthetic factors. The effectiveness of X11 to remove these impurities was assessed at the optimum conditions of FFA removal. The conditions were; contact time of 112 minutes, 7.5% (w/v) AC dosage, and a 240 rpm mixing speed.

4.7.1. PV Reduction

Lipid oxidation degrades oil quality since it forms primary products like hydro-peroxides. The PV is one of the measurements to quantify this oxidation. Under optimized conditions, the oil's initial PV was 29.31 meqO_2/kg. After AC treatment, the PV was decreased by 77.21% and it becomes 6.68 meqO_2/kg. This shows clear effectiveness of the AC for the adsorption of oxidation product.

4.7.2. Color Removal

Color is also another parameter that significantly impacts oil quality. Lightness of the UCO was measured using the L^* value. Initially, the UCO had an L^* value of 25.17. After treatment, the L^* value rose to 28.68. The change in L^* indicates that color pigments are effectively adsorbed by the PET-derived AC, X11.

4.8. Physicochemical Characteristics of UCO After Treatment

The untreated UCO was characterized after carrying out the adsorption operation at optimal FFA removal conditions. The FFA as oleic acid, the PV, and the color lightness were measured after the treatment. Table 4.12. summarizes the characterization results.

Table 4.12: Physicochemical and sensory properties of UCO before and after treatment

Parameter	Unit	Before Treatment	After Treatment
FFA	% oleic acid	1.2860	0.4089
PV	mgO_2/kg	29.3100	6.6800
Color lightness (L^*)	-	25.1700	28.6800

The visual appearance of the UCO before and after treatment is shown in the Figure 4.13 below.

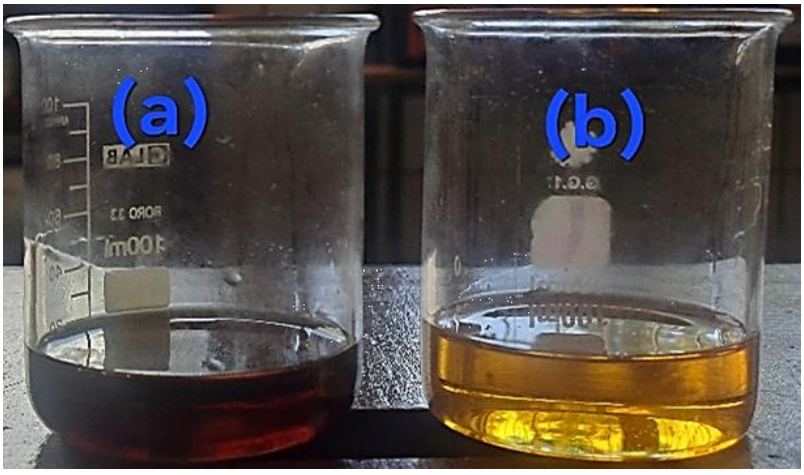

Figure 4.13: UCO (a) before and (b) after treatment

4.9. Comparative Analysis with Previous Studies

A comparison between the performance of X11 and other biomass-derived ACs in purifying UCO was done. The comparison focused on the FFA removal and the peroxide value reduction efficiencies since they are primary oil quality indicators (Jasmidi et al., 2023). However, the studies were conducted under different experimental conditions. Despite these differences, the comparison provides a general perspective on the performance of the PET-based AC compared to other biomass-based ACs. The summary of these results is presented in Table 4.13.

Table 4.13: Comparison of PET-derived AC with other biomass-based adsorbents in terms of FFA and PV reduction efficiency

AC Precursor	**Condition**			**Reduction Efficiency (%)**		**Reference**
	Temperature (°C)	Adsorbent Dose (%(w/v))	Contact time (min)	FFA	PV	
PET	Ambient	7.50	112	68.20	77.21	This study
Coconut Shell	-	5.00	15	37.50	85.40	Khuzaimah & Eralita, 2020
Cocoa Pod Husk	-	15.00	120	49.40	-	Arman et al., 2024
Bamboo	-	1.33	120	65.90	62.80	Suryandari & Kusuma, 2021
Rice Straw	35	15.00	60	40.78	5.05	Francisco & Villalobos, 2024
Banana Peel	-	2.00	60	54.38	-	Channei et al., 2025
Palm Empty Bunches	-	10.00	120	46.90	80.20	Jasmidi et al., 2023

Even though the treatment conditions are not identical, the comparison underscores the remarkable ability of PET-derived AC (X11) in UCO treatment. The AC performs both the removal of FFA (68.2% removal) and reduction of peroxide value (77.21% reduction).

5. Conclusions and Recommendations

5.1. Conclusion

AC was prepared from waste PET bottles through a two-stage chemical activation process, maintaining an activator-to-precursor ratio of 1:1 in both stages. The resulting AC exhibited significant characteristics, which were analyzed using BET, BJH, XRD, FTIR, SEM, EDX, and TGA techniques. It demonstrated a SSA of 984.9 m^2/g and a well-developed pore structure, along with essential surface functional groups suitable for its intended application.

Based on prior research, three factors were selected and optimized for FFA removal efficiency. The optimal adsorption conditions identified through BBD included a contact time of 111.72 minutes, an AC dosage of 7.49% (w/v), and a mixing speed of 236.21 rpm. With these optimal conditions, a maximum FFA removal efficiency of 68.2% was achieved. The kinetic studies resulted a correlation coefficients (R^2) of 0.9657 for PSO, 0.9644 for PFO, and 0.9522 for IPD models. The close values of R^2 may be an indicator that physical, chemical, and diffusional adsorption took place sequentially. However, the slightly higher R^2 for the PSO model indicates that chemical adsorption is the dominant mechanism.

Additionally, the AC was effective in significantly reducing the PV, color, and odor of the oil. The PV decreased from 29.31 meqO2/kg to 6.68 meqO2/kg, while the lightness of the oil changed from an L^* value of 25.17 to 28.68. Comparative analysis shows that PET-derived ACs can be as effective, or even superior, to other biomass-based ACs in treating UCO. Therefore, the AC X11 is recognized as a sustainable innovation for oil purification.

5.2. Recommendations

This study concludes that the PET-based AC was successful in removing FFAs and other impurities in a UCO sample. However, more optimization is needed to take this approach to full-scale. Ultimately, the following recommendations are made to guide future research and promote the adoption of the current findings in practice.

Firstly, carbonization and activation were carried out in an oxygen environment furnace. Even if the crucibles were covered, creating 100% oxygen free condition was unrealistic. Therefore, it is necessary to perform all the experiments using furnaces with precisely controlled inert atmospheres.

Secondly, this study focused on reducing limited number of impurities. While these impurities are important parameters that define oil quality, but they are not the only components. Thus, it is advisable to continue researching the reduction of other parameters such as viscosity and specific polar compounds.

Thirdly, to further confirm the sustainability of the proposed method, future studies should include Environmental Impact Assessments (EIA) and Life Cycle Assessments (LCA). The assessments should focus on resource usage, emissions, and environmental trade-offs related to the large-scale manufacturing.

Fourthly, this study was conducted at a laboratory scale and did not evaluate the economic feasibility of scaling up. Therefore, pilot or industrial-scale studies are needed to assess cost-effectiveness, operational challenges, and real-world applicability in continuous systems.

In addition, although optimization and kinetic studies were conducted, future research should also report adsorption capacity (e.g., mg FFA per g AC) to enable meaningful comparisons with other adsorbents and guide further improvements.

Lastly, for this research, fresh adsorbents were used for each run. But, this is neither sustainable nor economical for large-scale application. Therefore, future research should focus on the regeneration and reuse of adsorbents to ensure economic and environmental viability.

References

Abdul Hamid, N. S., Che Malek, N. A., Mokhtar, H., Mazlan, W. S., & Mohd Tajuddin, R. (2016). Removal of oil and grease from wastewater using natural adsorbents. Jurnal Teknologi, 78(5–3), 97–102. https://doi.org/10.11113/jt.v78.8519

Abdul Khalil, H. P. S., Jawaid, M., Firoozian, P., Rashid, U., Islam, A., & Akil, H. M. (2013). AC from various agricultural wastes by chemical activation with KOH: Preparation and characterization. Journal of Biobased Materials and Bioenergy, 7(6), 708–714. https://doi.org/10.1166/jbmb.2013.1379

Abrante-Pascual, S., Nieva-Echevarría, B., & Goicoechea-Oses, E. (2024). Vegetable Oils and Their Use for Frying: A Review of Their Compositional Differences and Degradation. Foods, 13(24). https://doi.org/10.3390/foods13244186

African Association of Entrepreneurs. (2020). Solid waste management and recycling in Ethiopia. https://aaeafrica.org/ethiopia/solid-waste-management-and-recycling-in-ethiopia/

Alabi-Babalola, O., Aransiola, E., Asuquo, E., Garforth, A., & D'Agostino, C. (2024). Production of Highly Efficient ACs for Wastewater Treatment from Post-Consumer PET Plastic Bottle Waste. ChemPlusChem, 89(5). https://doi.org/10.1002/cplu.202300484

Ali, E., Tahereh, K., & Mansooreh, S. (2014). Preparation of high surface area AC from Polyethyleneterephthalate (PET) waste by physical activation June 2011. https://www.researchgate.net/profile/Ali_Esfandiari/publication/233747899_Preparation_of_high_surface_area_activated_carbon_from_Polyethyleneterephthalate_PET_waste_by_physical_activation/links/09e4150b0f89da479e000000/Preparation-of-high-surface-area-act

Arman, A., Sukmawati Arifin, A., Hasizah Mochtar, A., & Irsaulul Nurhisna, N. (2024). Application of AC from Cocoa Pod Husk (Theobroma cacao L.) in UCO. BIO Web of Conferences, 96. https://doi.org/10.1051/bioconf/20249601032

Azzena, U., Montenero, A., Carraro, M., Crisafulli, R., De Luca, L., Gaspa, S., Muzzu, A., Nuvoli, L., Polese, R., Pisano, L., Pintus, E., Pintus, S., Girella, A., & Milanese, C. (2023). Recovery, Purification, Analysis and Chemical Modification of a Waste Cooking Oil. Waste and Biomass Valorization, 14(1), 145–157. https://doi.org/10.1007/s12649-022-01845-3

Balamurugan, G., Mohammed Rafi, I., & Nadu, T. (2021). An Experimental Study on Plastic Paver Tiles. International Journal of Innovative Research in Science, 10(5), 4297. https://doi.org/10.15680/IJIRSET.2021.1005023

Beghetto, V. (2025). Waste Cooking Oils into High-Value Products : Where Is the Industry Going ? 1–19.

Blanchard, R., & Mekonnen, T. H. (2024). Applied Polymers activation and carbonization into AC for functional material applications. 557–582. https://doi.org/10.1039/d4lp00016a

Bostan, R., Glevitzky, M., Varvara, S., Dumitrel, G. A., Rusu, G. I., Popa, M., Glevitzky, I., & Vică, M. L. (2024). Utilization of Natural Adsorbents in the Purification of Used Sunflower and Palm Cooking Oils. Applied Sciences (Switzerland), 14(11). https://doi.org/10.3390/app14114417

Dali, N., Dali, S., Chairunnas, A., Amalia, H. A. M., & Puspitasari, S. A. A. (2023). Pretreatment of UCO Using Avocado Seed Adsorbent for Biodiesel Production Preparation. Metana, 19(1), 44–52. https://doi.org/10.14710/metana.v19i1.51797

De Castro, C. S., Viau, L. N., Andrade, J. T., Mendonça, T. A. P., & Gonçalves, M. (2018). Mesoporous AC from polyethyleneterephthalate (PET) waste: Pollutant adsorption in aqueous solution. New Journal of Chemistry, 42(17), 14612–14619. https://doi.org/10.1039/c8nj02715c

Dhaka, V., Singh, S., Anil, A. G., Sunil Kumar Naik, T. S., Garg, S., Samuel, J., Kumar, M., Ramamurthy, P. C., & Singh, J. (2022). Occurrence, toxicity and remediation of PET plastics. A review. Environmental Chemistry Letters, 20(3), 1777–1800. https://doi.org/10.1007/s10311-021-01384-8

Efimov, M., Vasilev, A., Muratov, D., Panin, A., Malozovskaya, M., & Karpacheva, G. (2024). Application of Infrared Pyrolysis and Chemical Post-Activation in the Conversion of PET Waste into Porous Carbons for Water Purification. Polymers, 16(7). https://doi.org/10.3390/polym16070891

Francisco, M. C., & Villalobos, M. C. (2024). Rice Straw as an Adsorbent for Reducing the Peroxide and Acid Values of UCO. Chemical Engineering Transactions , 114(December), 1093–1098. https://doi.org/10.3303/CET24114183

Gao, L., Zhao, X., Zheng, X., Zhu, Y., & Cheng, J. (2018). Preparation of ACs from Waste External Thermal-Insulating Phenolic Foam Boards. MATEC Web of Conferences, 142. https://doi.org/10.1051/matecconf/201714201005

Geyer, R., Jambeck, J. R., & Law, K. L. (2017). Production, use, and fate of all plastics ever made. Science Advances, 3(7), 25–29. https://doi.org/10.1126/sciadv.1700782

Gustaman, F., Putri, R., … W. R.-R. J., & 2021, undefined. (2020). Community Empowerment To Purify UCO From Active Carbon Banana Peels In Pakintelan Village. Journal.Unnes.Ac.Id,18(2),30–35.

Harianingsih, H., Dyah Pita Rengga, W., Rihadatul 'Aisy Qothrun Nada, A., Ria Ramadhani, R., Syauqi, A., & Wulandari, R. (2023). Isothermal Adsorption of UCO Purification Using Avocado Seed Adsorbent. Jurnal Bahan Alam Terbarukan, 12(1), 45–51. https://doi.org/10.15294/jbat.v12i1.42247

Heidarinejad, Z., Dehghani, M. H., Heidari, M., Javedan, G., Ali, I., & Sillanpää, M. (2020). Methods for preparation and activation of AC: a review. Environmental Chemistry Letters, 18(2), 393–415. https://doi.org/10.1007/s10311-019-00955-0

Hendi, E. S., Rusdi, R., Alam, B. N., & Nurbaeti, S. (2021). Purification of UCO by Alkali Neutralization and Bleaching of Bayah Natural Zeolite. Jurnal Bahan Alam Terbarukan, 10(1), 36–42. https://doi.org/10.15294/jbat.v10i1.28636

Hiraga, K., Taniguchi, I., Yoshida, S., Kimura, Y., & Oda, K. (2019). Biodegradation of waste PET . EMBO Reports, 20(11), 1–5. https://doi.org/10.15252/embr.201949365

Ho, Y. S., & McKay, G. (1998). A Comparison of chemisorption kinetic models applied to pollutant removal on various sorbents. Process Safety and Environmental Protection, 76(4), 332–340. https://doi.org/10.1205/095758298529696

Ilgen, O., & Dulger, H. S. (2016). Removal of oleic acid from sunflower oil on zeolite 13X : Kinetics , equilibrium and thermodynamic studies. 81, 66–71.

Jagtoyen, M., & Derbyshire, F. (1998). Activated carbons from yellow poplar and white oak by H_3PO_4 activation. *Carbon, 36*(7–8), 1085–1097. https://doi.org/10.1016/S0008-6223(98)00082-9

Jamal, Y., & Boulanger, B. O. (2010). Separation of Oleic Acid from Soybean Oil Using Mixed-Bed Resins. 1000 mL, 2405–2409.

Jambeck, J. R., Geyer, R., Wilcox, C., Siegler, T. R., Perryman, M., Andrady, A., Narayan, R., & Law, K. L. (2015). Entradas de residuos plásticos desde la tierra al océano. Ciencia, 347http://www.sciencemag.org/cgi/doi/10.1126/science.1260879%0Ahttps://www.sciencemag.org/lookup/doi/10.1126/science.1260352

Jasmidi, J., Adelila Sari, S., Nizam, M., Zubir, M., Selly, R., Rahmah, S., Faradilla, P., Puspita Sari, D., & Fadhilah Husna, A. (2023). Improving UCO quality with adsorption of Fe-Cu AC derived from oil palm empty bunches. The 9th Annual International Seminar on Trends in Science and Science Education (AISTSSE) 2022, 0, 159–167. https://doi.org/10.2478/9788367405195-024

Jumiati, E. (2024). Refinement of cooking oil using AC from coconut shell and zeolite. Jurnal Teknosains, 13(2), 152. https://doi.org/10.22146/teknosains.91766

Karume, I., Bbumba, S., Tewolde, S., Mukasa, I. Z. T., & Ntale, M. (2023). Impact of carbonization conditions and adsorbate nature on the performance of AC in water treatment. BMC Chemistry, 17(1), 1–12. https://doi.org/10.1186/s13065-023-01091-1

Khuzaimah, S., & Eralita, N. (2020). Utilization of Adsorbent Carbon Coconut Shell for Purification of UCO. IJCA (Indonesian Journal of Chemical Analysis), 3(2), 88–95. https://doi.org/10.20885/ijca.vol3.iss2.art7

Kogyo Co, K. (2024). Federal Democratic Republic of Ethiopia Solid Waste Management Advisor for Addis Ababa City Project Completion Report Federal Democratic Republic of Ethiopia Addis Ababa Cleansing Management Agency. April.

Kuptajit, P. (2021). Development of Fast Activation Method using Microwave-Induced Plasma for Preparation of High-Surface-Area AC(Dissertation) Development of Fast Activation Method using Microwave-Induced Plasma for Preparation of High-Surface-Area AC. https://doi.org/10.14989/doctor.k23517

Laranjeira, C. M. C., Ventura, C. S. E., Bermejo, S. M. C. S., Santos, S. P. T. A. dos, Ribeiro, M. F. da S. P., Basto de Lima, M. G. de O. L., & Henriques, M. O. I. (2017). Used food oils: physical-chemical indicators of quality degradation. 154–159. https://doi.org/10.22616/foodbalt.2017.040

László, K., & Szucs, A. (2001). Surface characterization of polyethyleneterephthalate (PET) based AC and the effect of pH on its adsorption capacity from aqueous phenol and 2,3,4-trichlorophenol solutions. Carbon, 39(13), 1945–1953. https://doi.org/10.1016/S0008-6223(01)00005-7

Lebreton, L., & Andrady, A. (2019). Future scenarios of global plastic waste generation and disposal. Palgrave Communications, 5(1), 1–11. https://doi.org/10.1057/s41599-018-0212-7

Legesse, A. (2020). Preparation of Laundry Soap from UCOs: Getting value out of waste. Scientific Research and Essays, 15(1), 1–10. https://doi.org/10.5897/sre2019.6649

Mendoza-Carrasco, R., Cuerda-Correa, E. M., Alexandre-Franco, M. F., Fernández-González, C., & Gómez-Serrano, V. (2016). Preparation of high-quality AC from polyethyleneterephthalate (PET) bottle waste. Its use in the removal of pollutants in aqueous solution. Journal of Environmental Management, 181, 522–535. https://doi.org/10.1016/j.jenvman.2016.06.070

Ioannidou, O., & Zabaniotou, A. (2007). Agricultural residues as precursors for activated carbon production—A review. Renewable and Sustainable Energy Reviews, 11*(9)*, 1966–2005. https://doi.org/10.1016/j.rser.2006.03.013

Lua, A. C., & Guo, J. (1999). Activated carbon prepared from oil-palm stone by one-step CO_2 activation for gaseous adsorption. Carbon, 37(9), 1415–1421. https://doi.org/10.1016/S0008-6223(98)00341-4

Lua, A. C., & Yang, T. (2004). Effect of activation temperature on the textural and chemical properties of potassium hydroxide activated carbon prepared from pistachio-nut shell. Journal of Colloid and Interface Science, 274(2), 594–601. https://doi.org/10.1016/j.jcis.2004.02.012

Marsh, H., & Rodríguez-Reinoso, F. (2006). Activated Carbon. Elsevier.

Miskah, S., Aprianti, T., Agustien, M., Utama, Y., & Said, M. (2019). Purification of UCO Using AC Adsorbent from Durian Peel. IOP Conference Series: Earth and Environmental Science, 396(1). https://doi.org/10.1088/1755-1315/396/1/012003

Molina-Sabio, M., & Rodríguez-Reinoso, F. (2004). Role of chemical activation in the development of carbon porosity. Colloids and Surfaces A: Physicochemical and Engineering Aspects, *241*(1–3), 15–25. https://doi.org/10.1016/j.colsurfa.2004.04.007

Muhammad, M., Kamar, I., Chandra, A. R., Shrestha, A., & Pandey, G. P. (2023). Use of Bentonite Adsorbent from Ujong Pacu for the Adsorption Free Fatty Acids from Crude Palm Oil. Journal of Renewable Energy, Electrical, and Computer Engineering, 3(2), 76. https://doi.org/10.29103/jreece.v3i2.12479

Muringayil Joseph, T., Azat, S., Ahmadi, Z., Moini Jazani, O., Esmaeili, A., Kianfar, E., Haponiuk, J., & Thomas, S. (2024). PET (PET) recycling: A review. Case Studies in Chemical and Environmental Engineering, 9(February). https://doi.org/10.1016/j.cscee.2024.100673

Nandiyanto, A. B. D., Ragadhita, R., & Fiandini, M. (2023). Interpretation of Fourier Transform Infrared Spectra (FTIR): A Practical Approach in the Polymer/Plastic Thermal Decomposition. Indonesian Journal of Science and Technology, 8(1), 113–126. https://doi.org/10.17509/ijost.v8i1.53297

Natural Resources Stewardship Programme. (2021). Introducing low-cost technology to improve PET collection in Addis Ababa. Natural Resources Stewardship Programme. Retrieved from https://nature-stewardship.org/uncategorized/introducing-low-cost-technology-to-improve-pet-collection-in-addis-ababa/

Nayak, P. K., Dash, U., Radha Krishnan, K., Mishra, B. K., & Rayaguru, K. (2017). Process Optimization for Minimizing Residual Free Fatty Acid Levels in Fried Mustard Oil: Isotherm and Kinetics Studies. Journal of Food Process Engineering, 40(3). https://doi.org/10.1111/jfpe.12426

Nisticò, R. (2020). PET (PET) in the packaging industry. Polymer Testing, 90. https://doi.org/10.1016/j.polymertesting.2020.106707

Njewa, J. B., Vunain, E., & Biswick, T. (2022). Synthesis and Characterization of ACs Prepared from Agro-Wastes by Chemical Activation. Journal of Chemistry, 2022. https://doi.org/10.1155/2022/9975444

Nurhazirah, W., Kamaruzaman, B., Sultan, P., Shah, I., Suhaili, N., & Zin, M. (2019). Recycle of UCO. International Professional Learning Communities in Education 2019, June 2019, 1–5. https://www.researchgate.net/publication/346875548

Nuru, Z., & Getachew, P. (2021). Improving the quality of used frying niger seed oil with adsorbent treatment. Heliyon, 7(4), e06748. https://doi.org/10.1016/j.heliyon.2021.e06748

Nurulain, S., Aziz, N. A., Najib, M. S., Salim, M. R., & Manap, H. (2021). A review of free fatty acid determination methods for palm cooking oil. Journal of Physics: Conference Series, 1921(1). https://doi.org/10.1088/1742-6596/1921/1/012055

Ojo, A. A., & Awogbemi, O. (2024). Physicochemical assessment of vegetable oil used to fry some Nigerian food items. 87.

Olanrewaju Alade, A., Paul Olasesan, I., Latifah Odofin, O., Ajibade, (2022). Review on Environmental Impact and Valourization of Waste Cooking Oil. Journal of Engineering and Technology, 16(1), 144–163. https://www.researchgate.net/publication/366618878

Onn, M., Muniandy, K., Zaiton, S. N. A., & Wahit, M. U. (2023). Free Fatty Acid Reduction in Used Frying Oil via Bio Adsorbent: A Short Review. Chemical Engineering Transactions, 106(August), 139–144. https://doi.org/10.3303/CET23106024

Pereira, L., Castillo, V., Calero, M., Blázquez, G., Solís, R. R., & Martín-Lara, M. Á. (2024). Insights into using plastic waste to produce ACs for wastewater treatment applications: A review. Journal of Water Process Engineering, 62(March). https://doi.org/10.1016/j.jwpe.2024.105386

Pham, T. H. T. (2023). Synthesis of AC from PET (PET) Plastic Waste and Its Application for Removal of Organic Dyes from Water. Non-Metallic Material Science, 5(1), 27–37. https://doi.org/10.30564/nmms.v5i1.5663

Phothong, K., Tangsathitkulchai, C., & Lawtae, P. (2021). The analysis of pore development and formation of surface functional groups in bamboo-based activated carbon during CO_2 activation. *Molecules*, *26*(18), Article 5641. https://doi.org/10.3390/molecules26185641

Putra, R. S., Julianto, T. S., Hartono, P., Puspitasari, R. D., & Kurniawan, A. (2014). Pre-Treatment of used-cooking oil as feed stocks of biodiesel production by using AC and clay minerals. International Journal of Renewable Energy Development, 3(1), 33–35.

https://doi.org/10.14710/ijred.3.1.33-35

Rahayu, S., Sulviani, R., Kurniati, T. H., Dianhar, H., Asharo, R. K., Subandrate, & Taher, Z. B. M. (2024). Physicochemical profile of UCO-based liquid hand soap with AC sugarcane bagasse bio adsorbent technology. AIP Conference Proceedings, 2982(1), 50042. https://doi.org/10.1063/5.0185129

Ramadhani, A. N., Malik, A. F., & Fitriana, W. R. (2023). Utilization of Wasted Cooking Oil and Essential Oil of Sweet Orange Peel (Citrus sinensis) as Aromatherapy Candles. Equilibrium Journal of Chemical Engineering, 7(2), 191. https://doi.org/10.20961/equilibrium.v7i2.80308

Rezki, B., Essamlali, Y., Aadil, M., Semlal, N., & Zahouily, M. (2020). Biodiesel production from rapeseed oil and low free fatty acid waste cooking oil using a cesium modified natural phosphate catalyst. RSC Advances, 10(67), 41065–41077. https://doi.org/10.1039/d0ra07711a

Rodríguez-Reinoso, F. (1997). The role of carbon materials in heterogeneous catalysis. *Carbon*, *36*(3), 159–175. https://doi.org/10.1016/S0008-6223(97)00173-5

Saleem, J., Shahid, U. Bin, Hijab, M., Mackey, H., & Mckay, G. (2019). Production and applications of ACs as adsorbents from olive stones. 775–802.

Salgado, M. D. F., Abioye, A. M., Junoh, M. M., Santos, J. A. P., & Ani, F. N. (2018). Preparation of AC from babassu endocarpunder microwave radiation by physical activation. IOP Conference Series: Earth and Environmental Science, 105(1), 0–13. https://doi.org/10.1088/1755-1315/105/1/012116

Santomasi, G., Todaro, F., Petrella, A., Notarnicola, M., & Thoden van Velzen, E. U. (2024). Mechanical Recycling of PET Multi-Layer Post-Consumer Packaging: Effects of Impurity Content. Recycling, 9(5). https://doi.org/10.3390/recycling9050093

Shahcheragh, S. K., Bagheri Mohagheghi, M. M., & Shirpay, A. (2023). Effect of physical and chemical activation methods on the structure, optical absorbance, band gap and urbach energy of porous AC. SN Applied Sciences, 5(12). https://doi.org/10.1007/s42452-023-05559-6

Soong, Y. H. V., Sobkowicz, M. J., & Xie, D. (2022). Recent Advances in Biological Recycling of PET (PET) Plastic Wastes. Bioengineering, 9(3), 1–27.

https://doi.org/10.3390/bioengineering9030098

Soonmin, H., & Kabbashi, N. A. (2021). Review On AC : Synthesis , Properties And Applications. 69(9), 124–139. https://doi.org/10.14445/22315381/IJETT

Sukmawati, S. H., & Sunarto, S. (2021). Utilization of Coffee Waste as Active Charcoal For Purification of Waste Cooking Oil. Indonesian Journal of Chemistry and Environment, 3(2), 29–38. https://doi.org/10.21831/ijce.v3i2.43510

Suryandari, E. T., & Kusuma, H. H. (2021). The synthesis of javanese bamboo charcoal for purifiying cooking oil. IOP Conference Series: Earth and Environmental Science, 1796(1). https://doi.org/10.1088/1742-6596/1796/1/012107

Tadda, M. A., Ahsan, A., Shitu, A., & Elsergany, M. (2016). A review on AC : process , application and prospects. August 2017.

Takeda, S., Lawtae, P., *et al.* (2023). Improving porous properties of activated carbon from carbon gel by the OTA method. *RSC Advances*, *13*, 14065–14077. https://doi.org/10.1039/D3RA01647A

Tesfaye., T. (2020). Environmental Impacts of disposable PET plastic bottle, The case of Water Bottling Companies in Addis Ababa, MSc Thesis,. Addis Ababa University, Ethiopia.

Thommes, M., Kaneko, K., Neimark, A. V., Olivier, J. P., Rodriguez-Reinoso, F., Rouquerol, J., & Sing, K. S. W. (2015). Physisorption of gases, with special reference to the evaluation of surface area and pore size distribution (IUPAC Technical Report). Pure and Applied Chemistry, 87(9–10), 1051–1069. https://doi.org/10.1515/pac-2014-1117

Virtanen, T., Rudolph, G., Lopatina, A., Al-Rudainy, B., Schagerlöf, H., Puro, L., Kallioinen, M., & Lipnizki, F. (2020). Analysis of membrane fouling by Brunauer-Emmet-Teller nitrogen adsorption/desorption technique. Scientific Reports, 10(1), 1–10. https://doi.org/10.1038/s41598-020-59994-1

Vuorte, M., Vierros, S., Kuitunen, S., & Sammalkorpi, M. (2020). Adsorption of impurities in vegetable oil: A molecular modelling study. Journal of Colloid and Interface Science, 571, 55–65. https://doi.org/10.1016/j.jcis.2020.03.012

Wirawan, S. K., Timotius, D., Nugraha, I. M., Restana, A., Anggara, A. L., & Hidayatullah, S. (2022). Kinetics and Adsorption Equilibrium Study of Free Fatty Acid (FFA) from Crude Palm Oil (CPO) on Anionic Resin. ASEAN Journal of Chemical Engineering, 22(1), 33–

41. https://doi.org/10.22146/ajche.70319

Wright, S. L., & Kelly, F. J. (2017). Plastic and Human Health: A Micro Issue? Environmental Science and Technology, 51(12), 6634–6647. https://doi.org/10.1021/acs.est.7b00423

Yahia, E. H., Serafin, J., Román-Martínez, M. C., Saidi, M., Gallego, A. R., Atlas, S., & Ouzzine, M. (2024). Valorization of argan paste cake waste: Enhanced CO2 adsorption on chemically AC. Journal of Analytical and Applied Pyrolysis, 181(July). https://doi.org/10.1016/j.jaap.2024.106637

Yahya, M. A., Al-Qodah, Z., & Ngah, C. W. Z. (2015). Agricultural bio-waste materials as potential sustainable precursors used for activated carbon production: A review. Renewable and Sustainable Energy Reviews, 46, *218–235*. https://doi.org/10.1016/j.rser.2015.02.051

Yuan, X., Lee, J. G., Yun, H., Deng, S., Kim, Y. J., Lee, J. E., Kwak, S. K., & Lee, K. B. (2020). Solving two environmental issues simultaneously: Waste PET plastic bottle-derived microporous carbons for capturing CO2. Chemical Engineering Journal, 397(May). https://doi.org/10.1016/j.cej.2020.125350

Yuliusman, Nasruddin, Sanal, A., Bernama, A., Haris, F., & Ramadhan, I. T. (2017). Preparation of AC from waste plastics PET as adsorbent in natural gas storage. IOP Conference Series: Materials Science and Engineering, 176(1). https://doi.org/10.1088/1757-899X/176/1/012055

Zhang, Y., Zhang, Z., Zheng, J., Peng, R., Chang, M., Hu, F., Wang, Y., Hu, H., & Ou, J. Z. (2024). Sequential double chemical activation of biochar enables the fast and high-capacity capture of tetracycline. Materials Chemistry Frontiers, January. https://doi.org/10.1039/d4qm00381k

Zhou, X. (2021). Research on Conversion of Waste PET into Value-Added Monomer replacing Landfill and Incineration for Environmental Pollution Control. IOP Conference Series: Earth and Environmental Science, 859(1). https://doi.org/10.1088/1755-1315/859/1/012097

Appendices

Appendix A: Design Expert Model Summary

Table A.1: Build information for the model

File Version	13.0.5.0		
Study Type	RSM	Subtype	Randomized
Design Type	BBD	Runs	17.00
Design Model	Quadratic	Blocks	No Blocks

Table A.2: Model summary statistics

Source	Std. Dev.	R^2	Adjusted R^2	Predicted R^2	PRESS	
Linear	6.11	0.7504	0.6928	0.6149	748.33	
2FI	6.95	0.7515	0.6024	0.2941	1371.65	
Quadratic	**1.40**	**0.9929**	**0.9838**	**0.9072**	**180.41**	**Suggested**
Cubic	0.8325	0.9986	0.9943		*	Aliased

Appendix B: Design Expert Model Equations

Table B.1: Coefficients in terms of coded factors

Factor	Coefficient Estimate	Df	Standard Error	95% CI Low	95% CI High	VIF
Intercept	61.56	1	0.6274	60.08	63.04	
A-Time	10.00	1	0.4960	8.83	11.17	1.0000
B-AC Dosage	8.88	1	0.4960	7.70	10.05	1.0000
C-Mixing Speed	-1.88	1	0.4960	-3.05	-0.7021	1.0000
AB	-0.1250	1	0.7015	-1.78	1.53	1.0000
AC	-0.5750	1	0.7015	-2.23	1.08	1.0000
BC	-0.4250	1	0.7015	-2.08	1.23	1.0000
A^2	-6.69	1	0.6837	-8.31	-5.08	1.01
B^2	-7.44	1	0.6837	-9.06	-5.83	1.01
C^2	-1.59	1	0.6837	-3.21	0.0242	1.01

Table B.2: Actual and coded model equations

Final Equation in Terms of Actual Factors		Final Equation in Terms of Coded Factors	
FFA Removal Efficiency	=	FFA Removal Efficiency	=
-73.66750		+61.56	
+0.997375	Time	+10.00	*A
+13.67333	AC Dosage	+8.88	*B
+0.321000	Mixing Speed	-1.88	*C
-0.001042	Time * AC Dosage	-0.1250	*AB
-0.000287	Time * Mixing Speed	-0.5750	*AC
-0.002833	AC Dosage * Mixing Speed	-0.4250	*BC
-0.004183	$Time^2$	-6.69	$*A^2$
-0.826944	$AC\ Dosage^2$	-7.44	$*B^2$
-0.000637	$Mixing\ Speed^2$	-1.59	$*C^2$

Appendix C: Laboratory Procedures (Photographs)

Figure C.1: Experimental procedures' photograph confirmations